CHALMERS
UNIVERSITY OF TECHNOLOGY

Accurate control of flexible link robot arm

Master's thesis in System, Control and Mechatronics

JIAMING GAO

Department of Electrical Engineering
CHALMERS UNIVERSITY OF TECHNOLOGY
Gothenburg, Sweden 2018

Master's thesis 2018

Accurate control of flexible link robot arm

Based on inverse dynamics feedforward with PI feedback control scheme

JIAMING GAO

CHALMERS
UNIVERSITY OF TECHNOLOGY

Department of Electrical Engineering
Division of Systems and Control
Mechatronics research group
Chalmers University of Technology
Gothenburg, Sweden 2018

Accurate control of flexible link robot arm
Based on inverse dynamics feedforward with PI feedback control scheme
JIAMING GAO

Supervisor: Yiannis Karayiannidis, Department of Electrical Engineering
External Supervisor: Torgny Brogårdh, ABB Group
Examiner: Yiannis Karayiannidis, Department of Electrical Engineering

Master's Thesis 2018
Department of Electrical Engineering
Division of System and Control
Mechatronics research group
Chalmers University of Technology
SE-412 96 Gothenburg
Telephone +46 31 772 1000

Cover: Space Station robotic arm known as Canadarm2 bends above Earth. (Photo source: NASA STS-114 Shuttle Mission Imagery).

Typeset in LaTeX
Gothenburg, Sweden 2018

Accurate control of flexible link robot arm
Based on inverse dynamics feedforward with PI feedback control scheme
JIAMING GAO
Department of Electrical Engineering
Chalmers University of Technology

Abstract

Modelling and control of flexible link robot arms is an emerging research area in both academia and industry since flexible manipulators are getting more and more attention. Many studies have been carried out to find an efficient method for controlling the flexible link robot arm and dealing with vibrations in the flexible link. This thesis presents a modelling and control approach for a flexible link robot arm. In order to derive simplified models that are not computationally demanding and can be used in an inverse dynamic control scheme, the lumped mass spring damper model is used to represent the flexible link and flexible joint. The spring damper model can simulate resonance and anti-resonance for the flexible link. Both the 2 mass spring damper model and the 3 mass spring damper model are investigated in this thesis. The flexible link robot arm system used in the thesis consists of the Quanser SRV02 Rotary servo base unit and an external link. Two types of external links are mounted on the Quanser SRV02 base unit: rigid link and flexible link. The frequency response of the physical system is obtained by giving sinusoidal input signals and measuring motor velocities. The experiment is carried out using the spring damper model and tried to match with the physical system frequency response corresponding to that of the frequency domain. Both friction and backlash effects are considered during the matching process. Then deriving the inverse dynamics of the matched model, the applied voltage can be computed by feedforward control. Together with a classical structure of PI feedback control, the inverse dynamics computed voltage feedforward control scheme is applied to control the physical system. The experiment results show that the proposed control scheme can obtain better control performance comparing with a pure PI feedback controller.

Keywords: Flexible link manipulator, Robot arm, Friction compensation, Spring damper model, PI feedback control, Feedforward compensation, Inverse dynamics.

Acknowledgements

I am grateful for all the support and help received during my work with this thesis. First thanks to my mentor Yiannis Karayiannidis gave me this opportunity to work on this thesis project. I appreciate his discussion and suggestions for my thesis work in each meeting time. His seriousness and rigor in science motivate me for a high-quality research.
Special thanks to Torgny Brogårdh to guide me to finish this project. His rich knowledge and experience gave me a lot of help and support for my thesis journey. I am very grateful to Torgny who can come to the laboratory for every time I faced a problem. His passion for the science encourages me to have the great enthusiasm for the research work and a great interest for the further research.
I am appreciated to Balázs Adam Kulcsár who allowed me to use his laboratory equipment to do my test. I also express my gratitude to Giuseppe Giordano to give me the access to the laboratory and Prithwick Parthasarathy to give some improvement comments for my report.
It's my pleasure to study at Chalmers University of Technology. I am enjoying the time of study at Chalmers. Thanks for all of my professors who gave me knowledge and inspirations. I also want to thank all of my classmates to learn and discuss together. At last, I thank for my family and friends support.

Jiaming Gao, Gothenburg, November 2017

Contents

List of Figures

List of Tables

1
Introduction

1.1 Background

Robotic manipulators are widely used to help humans in different fields involving dangerous and tedious works. Many robotic manipulators have a large stiffness to guarantee the end effector accuracy. However, this heavy rigid design leads to a large power consumption and speed limitation. Nowadays, more and more new concept robots appear to collaborate with humans. Currentlly, ABB YUMI robot and KUKA LBR iiwa robot are considered to be the safe options due to the robot design with light weight arms and transmissions. Actually, the studies of flexible link robot arm started as part of the space robot research. Due to the enormous launching cost, the space manipulators should be also as light as possible. The use of robot arms in the space research robots has encouraged the researchers to research for the advancement towards flexible link robot arm. In contrast to traditional rigid robotic manipulators, a flexible link robot arm has the benefits of: larger work volume, higher operational speed, lower energy consumption, safer operation, lower overall mass and in general lower general cost.[1] Figure 1.1 shows a single link flexible robot arm.

However, there is a big drawback for a flexible link robot arm: vibration problem. This is due to the fact that a flexible link has many vibration frequencies with finite values and it can cause serious tip deflection even under normal operating conditions. Thus the flexible link robot arm is difficult to obtain high accuracy when performing demanding tasks.[3]

To achieve the accuracy of positioning the flexible links' end tip or end-effector, the vibration should be very minimum or null during the movement. Precise mathematical models for the system may be required.

Most commonly the dynamic models of the flexible link are abridged to some finite dimensional models, such as the assumed mode method (AMM) or the finite element method (FEM). For the assumed mode model, the link flexibility is expressed by a truncated finite modal series. It is hard to find modes for links with non-regular cross sections and multi-link manipulators. The finite element method superposes the elastic deformation by a known rigid body motion. However, it requires lots of boundary conditions which are uncertain for the flexible link robot arm.[5] There is a simpler model for analysis: the lumped parameter model where flexible link is modeled as mass spring damper system.

To control the motion of the flexible link, there are several control schemes: computed torque control, adaptive control, neural network control, lead-lag control,

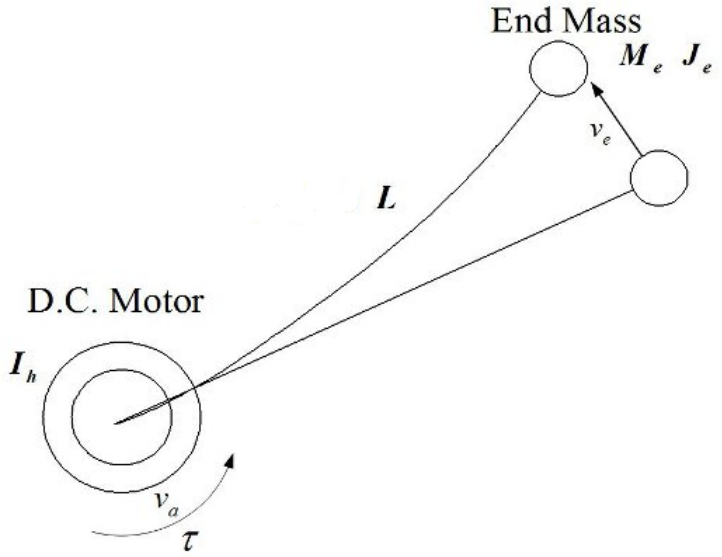

Figure 1.1: A model for single link flexible robot arm, where v_a is motor velocity, v_e is end-point velocity and τ is the control torque from the motor, I_h and J_e are motor and link inertia.[2]

sliding mode control, optimal and robust control etc. The control schemes can mainly be classified as feedforward control, feedback control or a combination of feedforward and feedback control. Feedforward control designs the control input to reduce the system vibration by taking care of the physical and vibration properties. Feedback control utilizes the measurements and estimates of the system states to lower the vibration.[5] A control scheme which combines the feedforward control and feedback control was investigated by Mazin Hamad.[6] Based on the lumped mass spring damper model, an inverse dynamics control and compensation schemes are presented in his report. However, the proposed control scheme was only tested in simulation.

This thesis aims to validate the proposed control scheme in practice. Considering joint flexibility incorporating friction and backlash, an inverse dynamics (based on mass spring damper model) feedforward with PI feedback control scheme is implemented and studied in the Quanser SRV02 rotary servo base unit.

1.2 Literature review

Many research works have investigated the modelling and control of the flexible link robot arms. Santosha and Peter[4] summarized most of the research work about the flexible link robot arm between 1974 to 2005. There are mainly three parts in the report: modeling, control and experiment. Benosman and Vey[7] presented more details for modelling and control of flexible link manipulators. Rigatos[8] conducted a comparative study on representative methods for model-based and model-free control of flexible-link robots.

1.2.1 Modelling of flexible link robot arm

The rigid link robot arm only has a finite number of degrees of freedom (DOF), which is usually expressed by ordinary differential equations. A flexible link robot arm that has an infinite number of degrees of freedom, needs to be modeled by partial differential equations. The work for modelling the flexible link robot arm can be divided into: assumed mode method, finite element method and lumped parameter method.
For the assumed mode model, the link flexibility is expressed by a truncated finite modal series with regard to spatial mode eigenfunctions and time-varying mode amplitudes. Cannon and Schmitz[9] investigated a flexible one link robot using the Lagrange's equation and the assumed mode method. Rakhsha and Goldenberg[10] proposed a model for a single link flexible robot using the Newton-Euler formulation and its natural frequencies and mode shapes are obtained using a constrained mode approach. Barbieri and Ozguner[11] derived a linear equation of motion of a flexible slewing link based on Hamilton's Extended Principle. They derived the finite Dimensional Models of the Slewing Beam using the assumed modes method.
There are many research works that focus on the finite element method. Bricout, Debus and Micheau[12] used the finite element method to analyze the flexible manipulators. The finite element method was combined with the Lagrangian formulation of the system motion. Moulin and Bayo[13] derived a single link flexible arm model using lumped finite element model, both the tracking order of the continuous model and discrete model were investigated. Mohamed and Tokhi[14] derived a constrained planar single-link flexible manipulator by the finite element method and developed a feedforward control scheme using command shaping techniques based on input shaping, low-pass and band-stop filtering to control the flexible link vibration.
Zhu, Ge and Lee[15] studied tip tracking control of a single-link flexible robot using the lumped model based on a spring-mass unit. A variation of the finite segment multi-body dynamics approach was proposed by Megahed and Hamza[16] to formulate the dynamic motion of planar flexible-link manipulators. Instead of the traditional lumped masses often encountered in the finite segment approach, the formulation used a consistent mass matrix in order to provide a better approximation. Khalil and Gautier[17] developed a method to model mechanical systems with flexible joints based on lumped elasticity model. Nissing[18] proposed a model independent approach for damping the vibrations of flexible robots. A spring damper element is attached to the flexible link. The actuators are controlled to reduce or remove the vibrations through optimizing the parameter configuration of the spring damper element.
There are also other studies for modeling the flexible link robot arm. For example, Asada, Park and Rai[19] investigated the structure and shape of flexible links that allow for fast, stable endpoint control.

1.2.2 Control of the flexible link robot arm

To control the flexible link robot arm, many control schemes have been employed. They are including: proportional derivative control, computed torque control, adaptive control, neural network based control, optimal and robust control, boundary

control and feedforward control etc.

Menq and Chen[20] designed a payload-adaptation controller of a flexible manipulator for tip position control. The payload-adaptation synthesizer integrated a payload identifier and a nominal estimator interpolator to get a LQG compensator. Feng and Palaniswami[21] designed a robust adaptive control algorithm for partially known continuous time systems with plant unmodelled dynamics and bounded disturbances and verified it in a single link flexible manipulator. Tzung-Cheng Yang,J.C.S. Yang and P. Kudva[22] proposed a new adaptive control scheme for a single-link flexible manipulator with unknown changing loads. The control scheme mainly contained a least-squares identification algorithm and a self tuning pole placement controller. Ji and Familoni[27] proposed a self-tuning control scheme for single link flexible manipulator system based on Recursive Least Square (RLS) parameter estimation method in time domain and Empirical Transfer Function Estimate (ETFE) in frequency domain.

Korolov and Chen[23] designed a class of robust controls for end-point position control problem of a one-link flexible manipulator. Based on the estimated state, the control scheme guaranteed the stability of the uncertain system and obtained better accuracy for the manipulator without the complete knowledge of the parameters. Misra[24] designed a robust control scheme for single link flexible manipulator under parameter uncertainties. Rattan and Feliu[25] developed a robust control scheme which based on two nested feedback loops to control the tip position of flexible manipulators with joint friction. The two feedback loops are: the inner loop controlling the position of the motor and the outer loop controlling the tip position.

Besides the adaptive and robust control strategies, there are also lots of other control schemes that were employed. Morgul[28] investigated a Boundary Control scheme for flexible beams. An optimal controller was designed by Pal, Stephanou and Cook[26] based on the state-space dynamic model for a manipulator with flexible links. Kotnik, Yurkovich and Ozguner[29] investigated three separate feedback control schemes: compensation using classical root locus techniques with endpoint position feedback, a full state feedback observer-based design, and compensation using endpoint acceleration feedback. Nader[30] designed a controller based on the original infinite dimensional distributed system for regulation of the angular displacement of the one-link flexible robot arm. This controller combined an additional on-line perturbation estimation to get rid of the effect of unmodeled dynamics and measurement defects. Gutierrez, Lewis and Lowe[31] presented a neural network (NN) tracking controller for a single flexible link robot. The practice implementation for this control method was showed much better tracking performance compared with PC and PID standard controllers.

Rattan and Feliu[32] designed the feedforward controllers to control the tip position of single-link flexible arms. The feedforward controller is by inverting the dynamics of the flexible link arm. Isobe and Kato[33] proposed a parallel solution scheme of inverse dynamics for flexible link system. The scheme derived the trajectories and torques values for feedforward control. A novel feedforward control scheme based on a PSO algorithm to the PTP motion of two flexible links for a flexible dual manipulator was proposed by Abe and Hashimoto[34]. This control method combined cycloidal and polynomial functions for the trajectory generation to smoothen the

trajectory and control the vibration.
The literature review on flexible link robot arm indicates that the dynamic analysis and control of flexible link robot arm is an emerging research area due to a wide spectrum of the applications in the field of automation, production and space robotics. Many cases used linearized model for model based control which can lower the complexity of controller. However, these control schemes can not take care of the large elastic deflection.[4] Most of the control schemes were only verified with simulation. Thus further experimental investigation is necessary to verify the theoretical studies. Further more, flexible joint incorporating friction and clearances should be considered in the experiment.

1.3 Objectives and Contributions

There are a lot of theoretical studies about how to control the flexible link robot arm. However, only few control schemes have been verified with experiment. This thesis focuses on the modelling of flexible link robot in order to derive simplified models that are not computationally demanding and can be used in inverse dynamic control scheme in dowel to a linear feedback controller. This thesis mainly investigates inverse dynamics computed voltage feedforward control with PI feedback control schemes and implements it for an experimental setup with motor and link flexibility. Padilla[35] investigated that using the end-point position to control joint actuation for the flexible manipulator will cause non-minimum phase behavior, which leads to limit the controller implementation and give rise to performance problems. Thus this thesis only makes use of the sensor feedback from the motor joint.
The objectives of this thesis are to:

- Investigate the mass spring damper system for modelling the flexible link robot arm system.
- Adapt a Quanser system both with respect to mechanics and control to perform control experiments
- Identify the parameters of the Quanser system to model dynamics, friction and backlash.
- Implement the inverse dynamics (based on mass spring damper model) feedforward computed voltage with PI feedback control scheme for the experimental setup
- Evaluate the control scheme based on experiment results

1.4 Thesis outline

This thesis work is organized as follows:
Chapter 2 Modeling of the flexible link robot arm introduces the laboratory equipment and the mathematical model for the flexible link robot arm. Both friction model and mass spring damper model are introduced to acquire a more accurate mathematical model for the flexible link robot arm system. It also explains how to obtain the frequency response of the physical model.

Chapter 3 Control system design illustrates the design theory of the control scheme for controlling the flexible link robot arm. Trajectory planning and filter design are also discussed this chapter.
Chapter 4 Results presents and discusses the experimental results. Different mass model are evaluated in this chapter.
Chapter 5 Conclusion and future work summarizes and concludes the experimental results. Future work is also discussed in this chapter.

2

Modeling of the flexible link robot arm

2.1 Quanser rotary servo base unit

2.1.1 Introduction for Quanser SRV02

The Quanser SRV02 rotary servo base unit, consists of a DC motor that is mounted on a solid aluminum frame and equipped with a planetary gearbox. The physical plant of the SRV02 unit is shown in figure 2.1. The motor has its own internal gearbox that drives external gears. Since this thesis work is trying to find the accurate model for the flexible link robot, the anti-backlash external planetary gearbox is used during the test. However, there exists a backlash inside the motor which can not be removed. The Quanser rotary servo base unit is equipped with three sensors: potentiometer, encoder, and tachometer. The tachometer is used to measure motor's velocity. The potentiometer and encoder are used to measure the external link angles.

Figure 2.1: The Quanser SRV02 rotary servo base unit.[36]

2.1.2 Mathematical model for the Quanser SRV02 system

The Quanser motor is a high efficiency, low inductance DC motor. To protect the motor, the input voltage is less than $15V$ and the input frequency should be limited to $50Hz$.
The DC motor armature circuit is shown in figure 2.2.

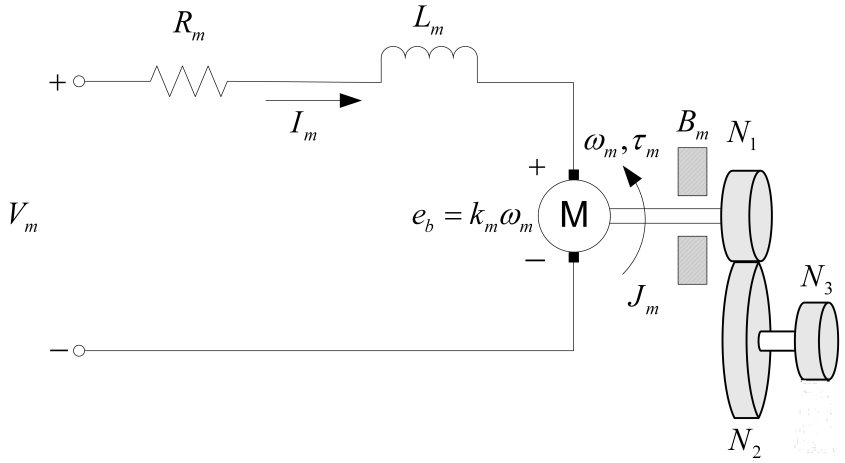

Figure 2.2: The Quanser motor armature circuit schematic, where R_m is the motor resistance, L_m is the inductance, k_m is the back-emf constant.[37]

From the figure 2.2, using the Kirchhoff's Voltage Law, the electrical equation is obtained as follow:

$$V_m - R_m I_m - L_m \frac{dI_m}{dt} - e_b = 0; \tag{2.1}$$

where V_m is the input voltage, I_m is the armature current and $e_b = k_m\omega_m$ is the back-emf (electromotive) voltage with ω_m and k_m being the motor speed and the back-emf constant respectively. Since the motor resistance is much larger than the motor inductance, the simplified electrical equation becomes:

$$V_m - R_m I_m - k_m\omega_m = 0; \tag{2.2}$$

For the one-degree rotary base unit, according to the Newton's Second Law, the mechanical equation is:

$$\tau_m = J_m \frac{d\omega_m}{dt} \tag{2.3}$$

where J_m is the motor inertia.
For the Quanser servo DC motor, the motor torque is proportional to voltage applied and described as[37]:

$$\tau_m = \eta_m k_t I_m \tag{2.4}$$

where η_m is the motor efficiency, k_t is the current-torque constant. Thus combining equation (2.2) and (2.4), the motor torque can be calculated by:

$$\tau_m = \eta_m k_t (\frac{V_m - k_m\omega_m}{R_m}) \tag{2.5}$$

The nominal value of the parameters are shown in table 2.1.

Table 2.1: Main specifications of the Quanser SRV02 rotary servo base unit.

Symbol	Definition	Value	Variation
R_m	Motor armature resistance	2.6Ω	$\pm 12\%$
L_m	Motor armature inductance	$0.18mH$	
k_t	Motor current-torque constant	$7.68 \times 10^{-3} Nm/A$	$\pm 12\%$
K_g	Motor gear ratio	14	
η_m	Motor efficiency	0.69	$\pm 5\%$
J_m	Motor moment of inertia	$4.606 \times 10^{-7} kg \cdot m^2$	$\pm 10\%$

2.2 Friction model

2.2.1 Friction model investigation

If there is no friction during the motor rotation, Eq (2.3) and (2.5) can be combined together to build the relation between input voltage and motor velocity. However, any mechanical system exhibits friction.To get a more accurate model, the friction effect should be investigated.

MATLAB SIMULINK is used to send different setpoint values of input voltage. The data is collected from the tachometer. Utilizing Eq (2.5), the motor torque is computed based on the nominal value from Quanser SRV02 specifications. For a constant motor velocity, the motor torque is assumed to be equal to the friction torque. Figure 2.3 shows the friction torque as a function of velocity.

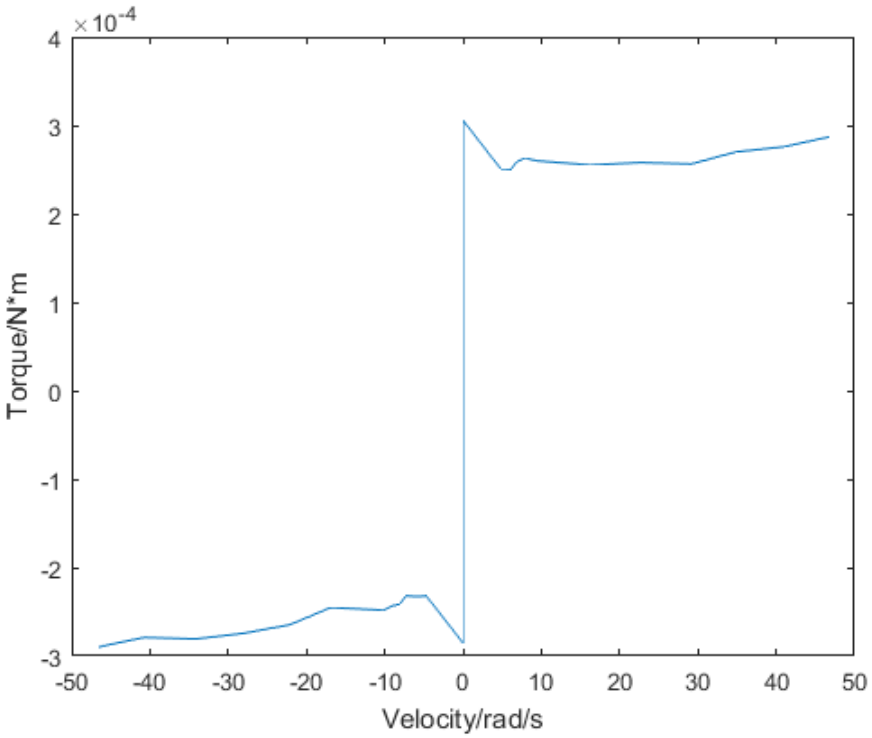

Figure 2.3: The plot between the friction torque and motor velocity.

In figure 2.3, the model of friction as a function of velocity is more like a Stribeck friction model.[38] In order to obtain uncomplicated inverse dynamic model for the feed-forward control, the model of friction is simplified to include the Coulomb friction and Viscous friction model as shown in figure 2.4. The friction model of the motor is:

$$\tau_{fm} = sign(\omega_m)\tau_{fc} + B_m\omega_m \tag{2.6}$$

where τ_{fc} is the Coulomb friction which is approximately $2.25 \times 10^{-4}Nm$ and B_m is the Viscous friction coefficient which is approximately $1.26 \times 10^{-6}Nm/(rad/s)$.

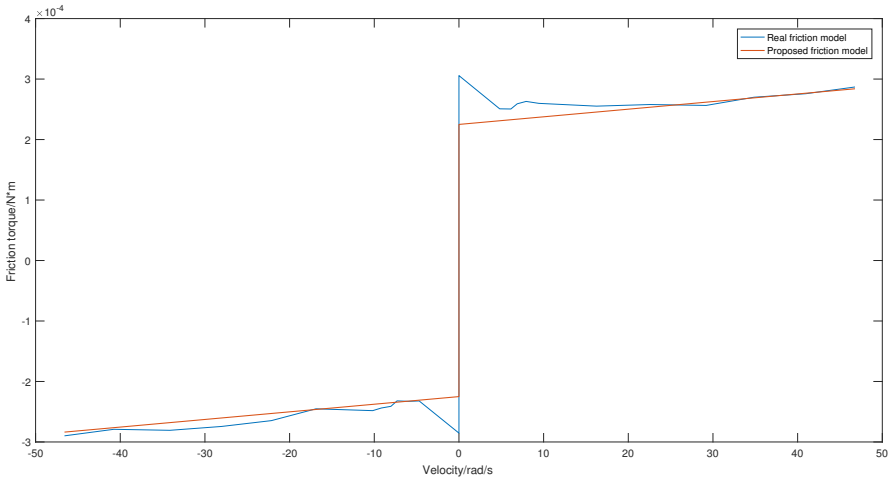

Figure 2.4: The plot of the proposed friction model comparing with the real friction model.

2.2.2 Friction model application

Considering the friction in the motor model, the mechanical equation (2.3) becomes:

$$\tau_m = J_m \frac{d\omega_m}{dt} + B_m \omega_m + \tau_{fc} \tag{2.7}$$

Combining the electrical equation (2.5) and mechanical equation (2.7) , the motor model can be expressed as:

$$\eta_m k_t \left(\frac{V_m - k_m \omega_m}{R_m}\right) = J_m \frac{d\omega_m}{dt} + B_m \omega_m + \tau_{fc} \tag{2.8}$$

Apply the Laplace transform for the Eq (2.8), the transfer function between the motor velocity and the input voltage becomes:

$$\frac{\omega_m}{V_m - \frac{R_m}{\eta_m k_t}\tau_{fc}} = \frac{\frac{\eta_m k_t}{R_m}}{J_m s + B_m + \frac{\eta_m k_t}{R_m} k_m} \tag{2.9}$$

By setting $V = V_m - sign(\omega_m)\frac{R_m}{\eta_m k_t}\tau_{fc}$, the motor system with output of the ω_m for and the input V is a first order time invariant system.

$$\frac{\omega_m}{V} = \frac{\frac{\eta_m k_t}{R_m}}{J_m s + B_m + \frac{\eta_m k_t}{R_m} k_m} \tag{2.10}$$

2.3 Frequency response identification

In order to acquire the characteristic of the dynamics of the physical system, frequency response should be analyzed regarding the Quanser SRV02 system. There are several methods to investigate system frequency response, such as impulse response, step response and sine wave response. Sine wave response is easier to operate

on the physical system. If a sinusoidal signal is injected into the system, the output has the same frequency for the linear time invariant system and for 'real' nonlinear processes the output will be approximately sinusoidal and will cycle with the input frequency.[39] For example, consider a sinusoidal signal as input:

$$u(t) = \alpha \sin(\omega t) \tag{2.11}$$

Then the resulting output is a sine wave with the same frequency but with a different amplitude:

$$y(t) = \alpha \mid G(e^{j\omega}) \mid sin(\omega t + \phi) \tag{2.12}$$

Given the different frequency of the input sine wave and measuring the resulting output, the frequency response of the system can be identified.[40]

2.3.1 Frequency response for only Quanser SRV02 system

In this thesis, the system frequency response can be derived by applying voltage inputs with different frequency and measuring the motor velocities from the tachometer. Figure 2.5 displays a plot between the input and measurement at frequency 1Hz.

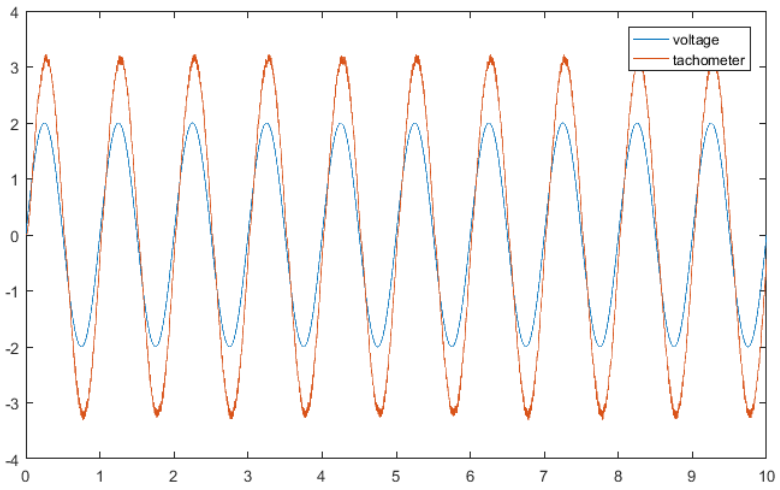

Figure 2.5: The input voltage and the measurements from the tachometer. The frequency of the input voltage is 1Hz. x axis is time and y axis is watt for the voltage. The measurement values of the tachometer also need multiplication with tachometer sensitivity to get exact motor value.

The magnitude bode plot of a system can be obtained by calculating all the gains at the varying frequency. Table 2.2 contains the collected data from the physical system with the frequency range from $0.1Hz$ to $8Hz$.

Table 2.2: Collected frequency response data for Quanser SRV02 Servo base unit.

Frequency(Hz)	Amplitude(v)	Maximum motor speed(rad/s)	Gain (db)
0.1	2	228.2891	41.6171
0.3	2	227.5909	41.5905
0.5	2	227.3815	41.5825
1	2	225.4965	41.5102
2	2	219.2134	41.2647
3	2	209.4395	40.8685
4	2	196.1750	40.3002
5	2	183.6086	39.7252
6	2	171.0423	39.1094
7	2	159.8722	38.5228
8	2	146.6077	37.7705

Figure 2.6 represents the comparison between the physical model and the proposed mathematical model. The proposed mathematical model is computed by taking the nominal value from the SRV02 unit specifications and the friction model values into Eq (2.10). Figure 2.6 proves that the proposed mathematical model has almost the same frequency response as the physical system.

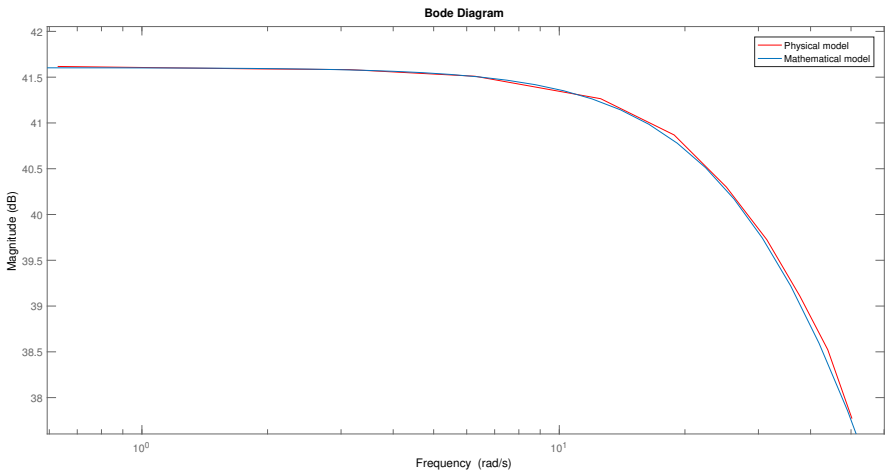

Figure 2.6: The comparison between the physical model and the proposed mathematical model for the Quanser SRV02 system.

2.3.2 Frequency response for Quanser SRV02 system with extra load

An extra load is added to the Quanser SRV02 system, note that different extra loads have the different inertias for the system. Giving the varying frequency of the input voltage, the frequency response for the different inertias can be found in the magnitude bode plot shown in figure 2.7

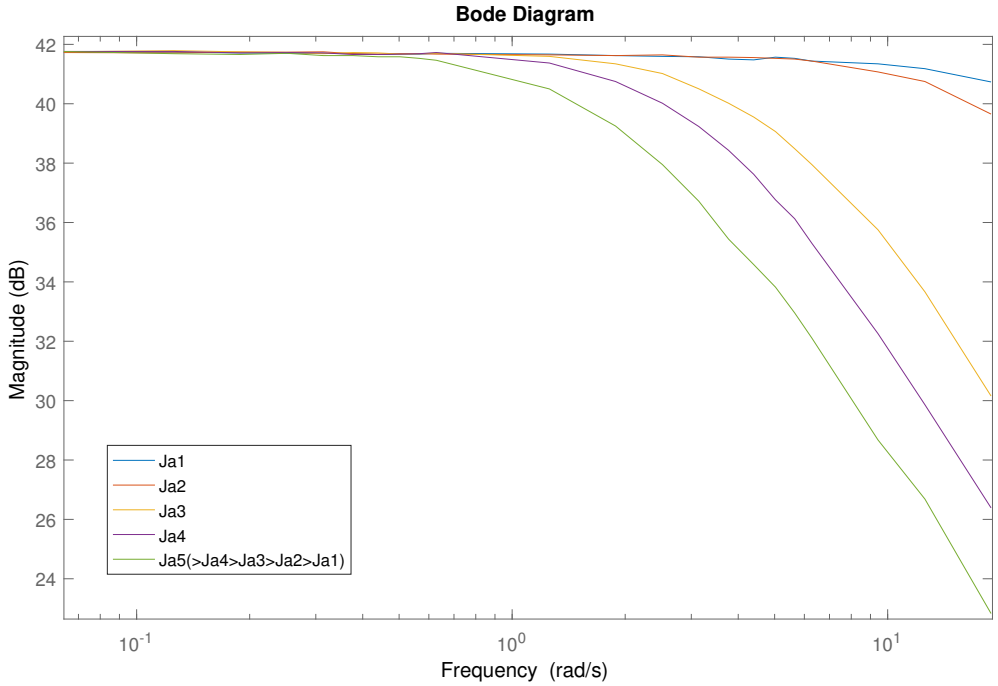

Figure 2.7: The frequency response of the Quanser SRV02 system with different extra load.

As the figure 2.7 shows, the large extra inertia can get more characteristic for the system frequency response. Since there is limited input frequency for the Quanser SRV02 system, a larger frequency range of input voltage is tested for the large extra load system. Figure 2.8 shows the bode plot with frequency from $0.01Hz$ to $50Hz$. The frequency responce of the system contains a resonance and a anti-resonance which may be caused by the backlash inside the motor internal gearbox of the Quanser system. Thus a flexible joint between extra load and motor should be considered in the system. As the figure 2.8 shows, the first order system can not fit the physical model frequency response. A new model should be introduced in the mathematical model.

2.4 Mass spring damper model for system

2.4.1 2 mass spring damper model

In this case, a 2-mass spring damper model is used to simulate the flexible joint. Figure 2.9 displays a simple 2 mass spring damper model. T_m and J_m are the motor torque and motor inertia, respectively k_a, d_a and J_a are the stiffness, damping and inertia or the flexible gearbox or the flexible link.

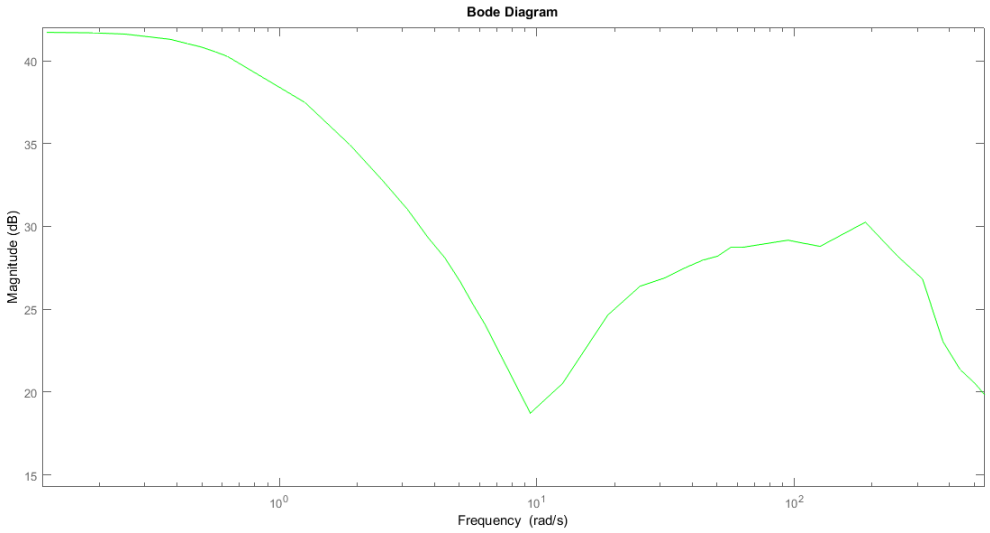

Figure 2.8: The frequency response of the large extra load Quanser SRV02 system with longer frequency range.

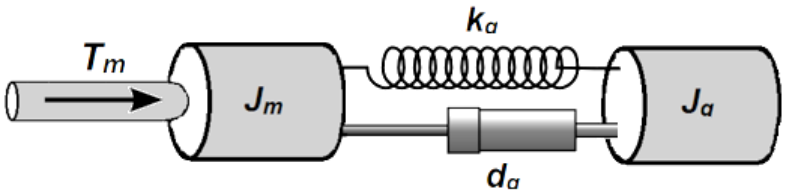

Figure 2.9: 2 mass spring damper model for a flexible link robot arm.[6]

According to the Newton's second law, the equations of mechanical system will become:

$$0 = J_a\ddot{\phi}_a + d_a(\dot{\phi}_a - \frac{1}{k_g}\dot{\phi}_m) + k_a(\phi_a - \frac{1}{k_g}\phi_m) + B_a\dot{\phi}_a \tag{2.13}$$

$$\tau_m = J_m\ddot{\phi}_m - k_g(d_a(\dot{\phi}_a - \frac{1}{k_g}\dot{\phi}_m) - k_a(\phi_a - \frac{1}{k_g}\phi_m)) + \tau_{fm} \tag{2.14}$$

where:
ϕ_m, ϕ_a: Motor angular position and the gearbox angular position(rad).
$\dot{\phi}_m, \dot{\phi}_a$: Motor angular speed and the gearbox angular speed(rad/s).
$\ddot{\phi}_m, \ddot{\phi}_a$: Motor angular acceleration and the gearbox angular acceleration(rad/s^2).
J_a: Gearbox(or flexible link) inertia($k_g \cdot m^2$).
k_g: Gearbox gear ratio.
k_a: Gearbox(or flexible link) stiffness(N/m).
d_a: Gearbox(or flexible link) damping(N/m^2).
B_a: Gearbox viscous friction(N/m^2).
τ_{fm}: Motor friction model($N \cdot m$).
Combining the electrical equation, the Quanser SRV02 system can be described as

the transfer function:

$$G(s) = \frac{\dot{\Phi}_m}{V} = \frac{a(J_a s^2 + (d_a + B_a)s + k_a)}{{}_m J_a s^3 + [J_a(B_m + ak_m + da) + J_m(da + B_a)]s^2 + [k_a(J_m + J_a) + d_a(B_m + B_a + ak_m) + B_a(B_m + ak_m)]s + k_a(B_m + B_a + ak_m)} \tag{2.15}$$

where $a = \frac{\eta_m k_t}{R_m}$.
Then matching the physical model frequency response by applying the proposed mathematical model of equation (2.15). After obtaining the matched results, the inverse dynamics model can be derived from the equations (2.13) and (2.14). The inverse model and feedforward computed compensation voltage for the 2 mass spring damper model are given below:

$$\begin{aligned} \phi_m^{ref}(s) &= \frac{k_g(J_a s^2 + (d_a + B_a)s + k_a)}{d_a s^2 + k_a} \dot{\phi}_a^{ref}(s) \\ \dot{\phi}_m^{ref}(s) &= s\phi_m^{ref}(s) \\ \ddot{\phi}_m^{ref} &= s\dot{\phi}_m^{ref} \\ V^{FFW} &= J_m \ddot{\phi}_m^{ref}(s) + \tau_{fm} + k_g(J_a \ddot{\phi}_a^{ref} + B_a \dot{\phi}_a^{ref}) \end{aligned} \tag{2.16}$$

2.4.2 3 mass spring damper model

If there is more resonance in the physical model, a 2 mass spring damper model can not get good matching results in the frequency domain. Thus a 3 mass spring damper model is necessary to be employed in order to achieve frequency matching. Figure 2.10 displays a simple 3 mass spring damper model. T_m,J_m, d_a, k_a and J_a are defined in the 2 mass spring damper model. k_l, d_l and J_l are the stiffness, damping and inertia of the flexible link.

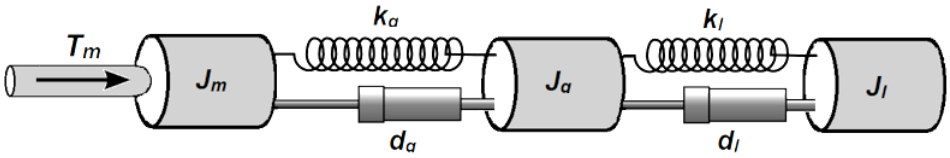

Figure 2.10: 3 mass spring damper model for a flexible link robot arm.[6]

For the 3 mass spring damper model, based on the Newton's law, the mechanical equation for the system is:

$$0 = J_l \ddot{\phi}_l + d_l(\dot{\phi}_l - \dot{\phi}_a) + k_l(\phi_l - \phi_a) + B_l \dot{\phi}_l \tag{2.17}$$

$$0 = J_a \ddot{\phi}_a + d_a(\dot{\phi}_a - \frac{1}{k_g}\dot{\phi}_m) + k_a(\phi_a - \frac{1}{k_g}\phi_m) - d_l(\dot{\phi}_l - \dot{\phi}_a) - k_l(\phi_l - \phi_a) \tag{2.18}$$

$$\tau_m = J_m \ddot{\phi}_m - k_g(d_a(\dot{\phi}_a - \dot{\phi}_m) - k_a(\phi_a - \phi_m)) + \tau_{fm} \tag{2.19}$$

where:
$\phi_m, \phi_a, k_g, J_a, d_a$ and k_a are defined as 2 mass spring damper model.

ϕ_l: The extra flexible link angular position(rad).
$\dot{\phi}_l$: The extra link angular speed(rad/s).
$\ddot{\phi}_l$: The extra link angular acceleration(rad/s^2)
J_l: The extra link inertia($k_g \cdot m^2$).
k_l: The extra link stiffness(N/m).
d_l: The extra link damping(N/m^2).
B_l: The extra link viscous friction(N/m^2)

Combining the electrical equation, the Quanser SRV02 system can be described by the transfer function:

$$G(s) = \frac{\dot{\Phi}_m}{V} = \frac{\begin{array}{r} a[J_a J_l s^4 + [J_a(d_l + B_l) + J_l(d_a + d_l)]s^3 + [J_a k_l + J_l(k_a + k_l) \\ + d_a(dl + B_l) + dlB_l]s^2 + [k_l(d_a + B_l) + k_a(d_l + B_l)]s + k_a k_l] \end{array}}{\begin{array}{r} J_m J_a J_l s^5 + [J_m J_a(d_l + B_l) + J_m J_l(d_a + d_l) + J_a J_l(d_a + B_m + a1k_m)]s^4 \\ +[J_m(J_a k_l + J_l(k_a + k_l + d_a(d_l + B_l) + d_l B_l) + (d_a + B_m + ak_m) \\ (J_a(d_l + B_l) + J_l d_l) + J_l d_l(B_m + ak_m)]s^3 + [J_m(k_l(d_a + B_l) \\ +k_a(d_l + B_l)) + (d_a + B_m + ak_m)(J_a k_l + J_l k_l + d_l B_l) + (B_m + ak_m) \\ (d_a(d_l + B_l) + J_l k_l) + k_a(J_a(d_l + B_l) + J_l d_l)]s^2 + [J_m k_l k_a \\ +(B_m + ak_m)(K_l(d_a + B_l) + k_a(d_l + B_l)) + d_a k_l B_l + k_a(J_a k_l \\ + J_l k_l + d_l B_l)]s + k_a k_l(B_m + B_l + ak_m) \end{array}} \tag{2.20}$$

The inverse model and feed forward computed compensation voltage for a 3 mass spring damper model are given as follow:

$$\begin{aligned}
\phi_a^{ref}(s) &= \frac{J_l s^2 + (d_l + B_l)s + k_l}{d_l s + k_l}\phi_l^{ref} \\
\dot{\phi}_a^{ref}(s) &= s\phi_a^{ref}(s) \\
\ddot{\phi}_a^{ref}(s) &= s\dot{\phi}_a^{ref}(s) \\
\phi_m^{ref}(s) &= \frac{k_g(J_a s^2 + (d_a + d_l)s + (k_a + k_l))}{d_a s + k_a}\phi_a^{ref}(s) + \frac{k_g(d_l s + k_l)}{d_a s + k_a}\phi_l^{ref}(s) \\
\dot{\phi}_m^{ref}(s) &= s\phi_m^{ref}(s) \\
\ddot{\phi}_m^{ref} &= s\dot{\phi}_m^{ref} \\
V^{FFW} &= J_m\ddot{\phi}_m^{ref}(s) + \tau_{fm} + k_g(J_a\ddot{\phi}_a^{ref} + J_l\ddot{\phi}_l^{ref} + B_l\dot{\phi}_l)
\end{aligned} \tag{2.21}$$

3

Control system design

3.1 Control scheme

For the high performance motion control, a combination of feedback and feedforward control is normally used and implemented in motion system.[43] The planning and execution in the computer hardware are composed of[44]:

- Trajectory planning: to calculate the acceptable path.
- Feedforward control: to calculate the input signal to improve tracking performance
- System compensation: to diminish and eliminate the disturbance and nonlinearity effect.
- feedback control: to ensure stability and to improve disturbance elimination.
- other issues: such as safety, diagnostics and communication, etc.

To execute all above tasks is hard for the motion controller. Typically a method called 'mass feedforward' or 'rigid body feedforward' is used to simplify these tasks. In this method, the trajectory planning and feedforward control are independent and separated with the actuating device. However, there are mainly two drawbacks when using the 'mass feedforward' method: a) if the actual position is too large during the trajectory execution, the actual input may be much larger than planned which could cause the problem for the actuator, and b) if the position error is still large after reaching the designed endpoint. The dynamic state of system needs time to settle down. To improve the control performance and try to avoid the aforementioned problems, three improvements for the aforementioned tasks are summarized as follows [45]:

- Trajectory smoothing or shaping: It can be achieved through reducing the acceleration and speed bounds for the trajectory planning. But it can also result in longer executing time.
- Feedforward control based on plant inversion: It requires either a more accurate model of motion system or learning the behaviour at the plant based on measurements.
- Feedback control optimization: Trying to improve the feedback control performance. It is also possible to add system compensation.

Figure 3.1 shows a simple control scheme for the flexible link robot arm.

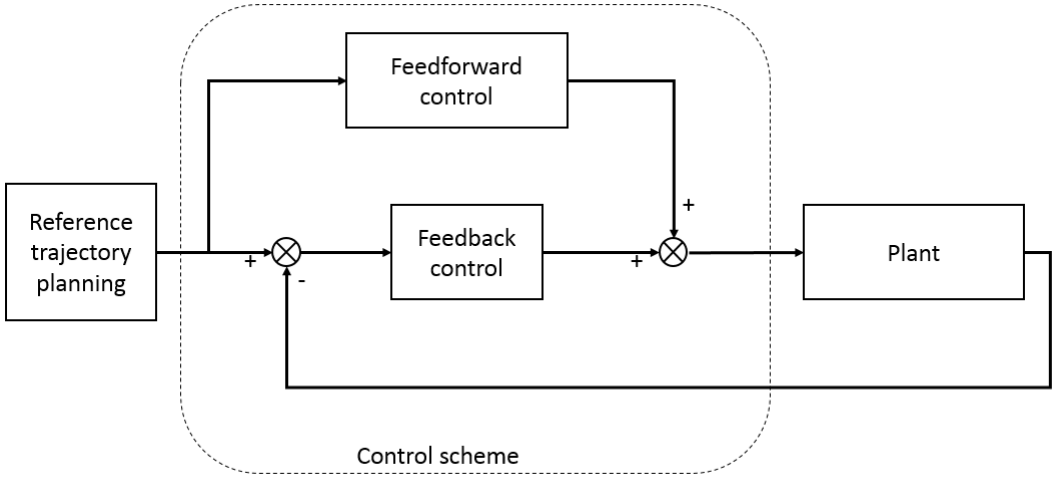

Figure 3.1: A general control scheme for flexible link robot arm.

3.2 Trajectory planning

Comparing with improving feedback control, the higher order trajectory is a more effective way to improve the motion control performance. This is because the higher-order trajectory lowers energy content which leads to lower error signal at high frequency. Higher-order trajectory also reduces the demands for motion which is difficult to perform for the physical actuator. These effects can be described as 'smoothing' which can reduce position error and settling time. The inverse dynamic model and feedforward controller have the following requirements for the reference trajectory: the 2 mass spring damper model requires that the motor acceleration is continuous and the 3 mass spring damper model requires that the derivative of the motor acceleration is continuous. Thus a fourth order trajectory planner is introduced and used for the experiment.

3.2.1 Fourth order trajectory planning

There are many ways to plan a fourth order trajectory.[46] Two types of the jerk which is the derivative of the acceleration can be chosen: trapezoidal or triangular jerk motion profiles. It is necessary to bound the maximum value of the jerk by defining its first derivative which is expressed by 'snap' or 'djerk'. Figure 3.2 shows two types of the choices.

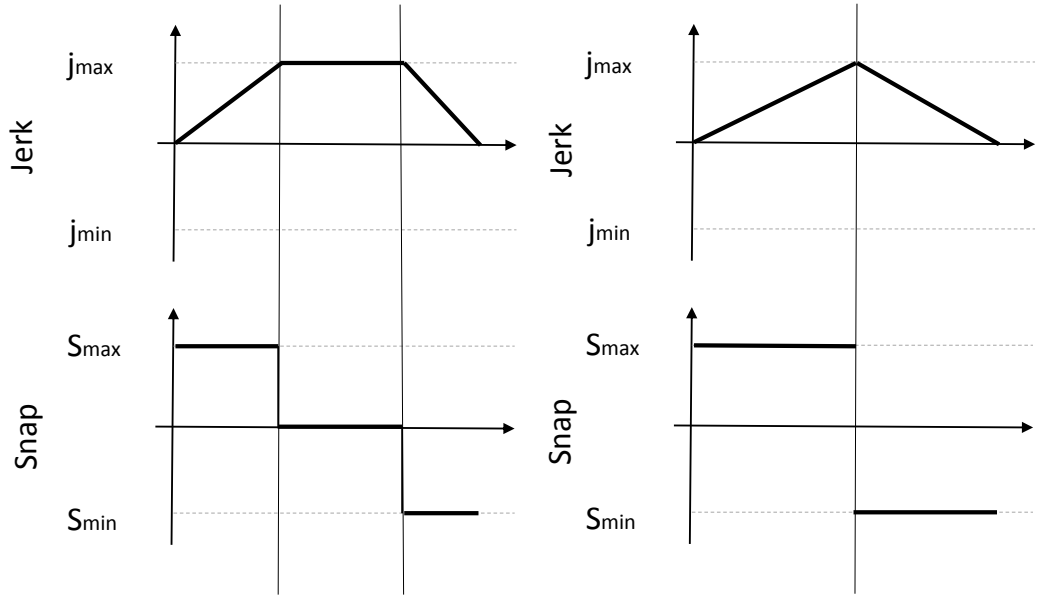

Figure 3.2: Two types of jerk model. Left graph is the trapezoidal jerk motion profile and right graph is the triangular jerk motion profile.

In the standard case, if the end position p_1 and the start position p_0 (where $p_1 > p_0$)are given, the velocity, acceleration, jerk and snap can be defined:

$$v_{max} = -v_{min}, a_{max} = -a_{min}, j_{max} = -j_{min}, s_{max} = -s_{min} \tag{3.1}$$

To simplify the trajectory planning, the triangular jerk motion profile is used for reference trajectory planning. The designed reference trajectory is depicted in figure 3.3. In figure 3.3, the boundary condition is $q_0 = 0, q_1 = 2.4, v_0 = 0, v_1 = 2.4$ with constrains $v_{max} = 2.4, a_{max} = 4.8, j_{max} = 19.2$ and $s_{max} = 76.8$. It is worth to mention that this reference trajectory is applied as trajectory 3 during the experiment.

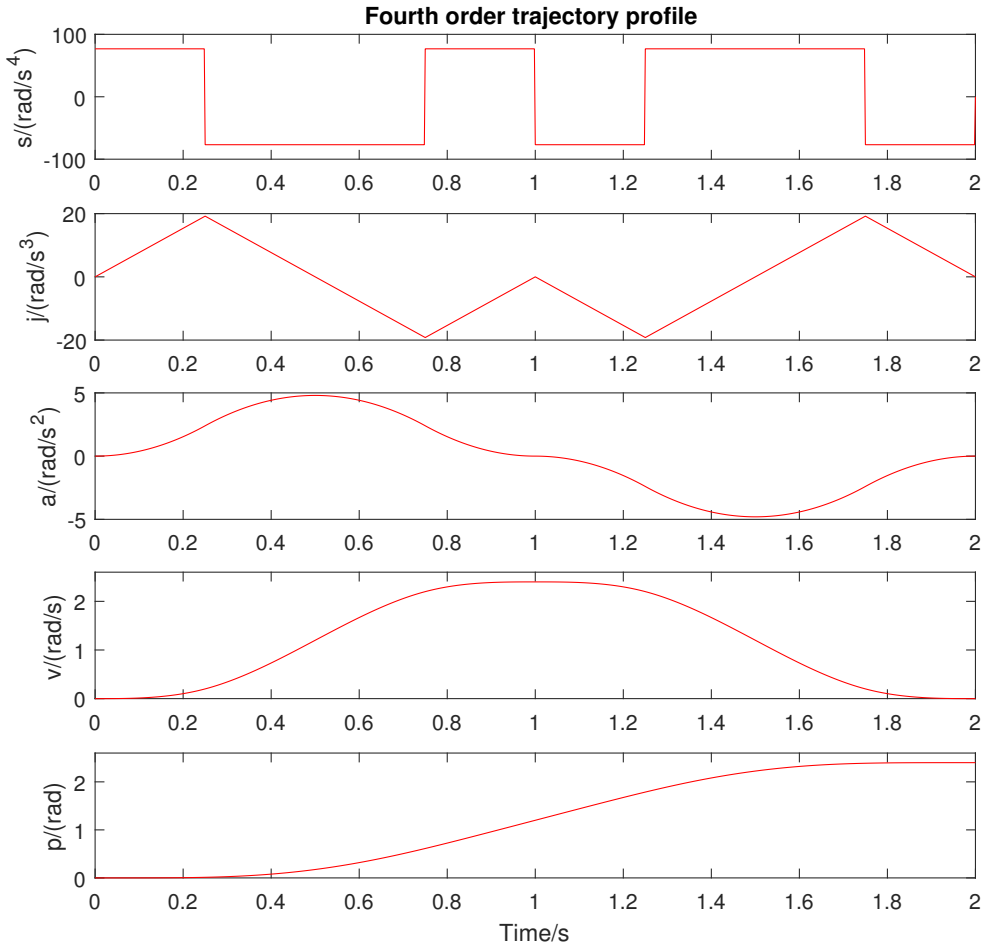

Figure 3.3: Fourth order trajectory which contains five segments: position p, velocity v, acceleration a, jerk j and snap s.

3.3 Frequency response matching

3.3.1 Backlash effects for the system frequency response

The backlash due to the motor gearbox can not be avoided, thus the effect of the backlash for the system should be investigated when analyzing the physical system.

J.H.Beak , Y.K.Kwak and S.H.Kim analyze the influence of the magnitude of the total backlash and the input voltage affect to the frequency response characteristic of the servo system.[41] A sinusoidal voltage was applied to the motor and the motor's angular velocity data was measured as output. Figure 3.4 shows how the frequency response of the servo system was affected by backlash.[42]

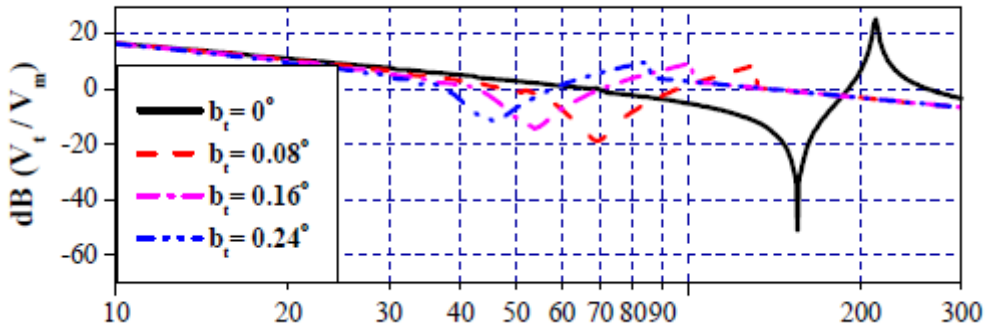

Figure 3.4: The frequency response of the servo system when different amplitude of backlash was applied. x axis is the frequency unit Hz, y axis is the system's gain where V_t is the motor's angular velocity and V_m is the input voltage.

Figure 3.4 reveals that the backlash of the gear reducer of the servo system reduces the effective equivalent torsion stiffness. Therefore, the anti-resonance and resonance frequency of the system are reduced. Since the accurate mathematical model is needed for controlling the physical system, the frequency response matching using the mass spring damper model should consider the backlash affect.

3.3.2 Frequency response matching for extra rigid link model

A large inertia extra rigid link is mounted in the Quanser SRV02 system. The frequency response of the extra rigid link model is derived following the procedure described in chapter 2.3. Figure 3.5 portrays the matching results by using 2 mass spring damper model in frequency domain. Note that the proposed 2 mass spring damper model is hard to match perfectly with the physical model frequency response. Considering the backlash effect in the system, the matched 2 mass spring damper model ought to increase the resonance and anti-resonance frequency during the matching process. The red line in figure 3.5 corresponds to the real matching results.

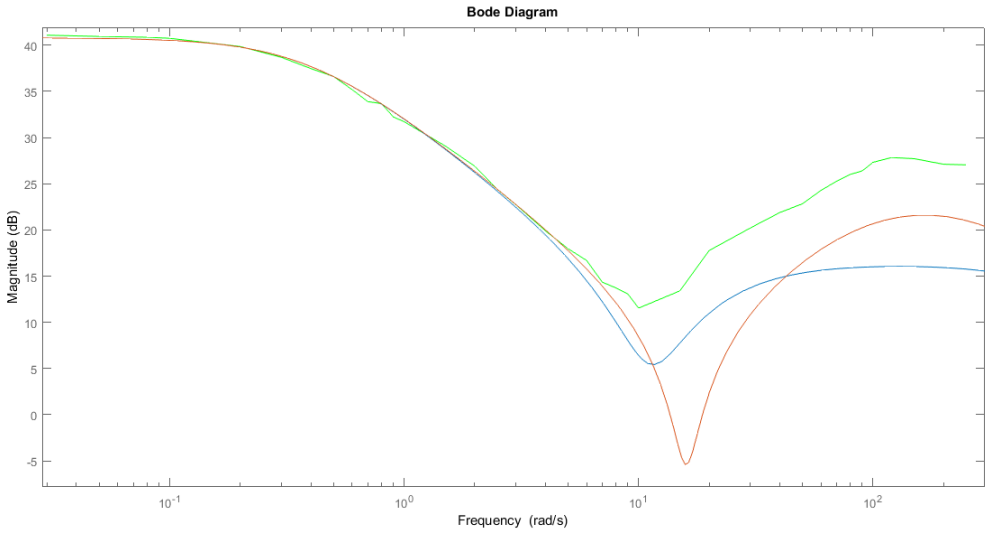

Figure 3.5: Frequency response matching plot using the 2 mass spring damper model. The green line is the extra rigid link physical model bode plot, the blue line is the 2 mass model matching plot without considering the backlash effects; the red line is the 2 mass model matching plot with considering the backlash effects.

3.3.3 Frequency response matching for extra flexible link model

A rigid link fixed by two springs composes the flexible link for the Quanser system. The frequency response of the extra flexible link model is depicted in Figure 3.6. Note that in this case there are two resonance frequencies.

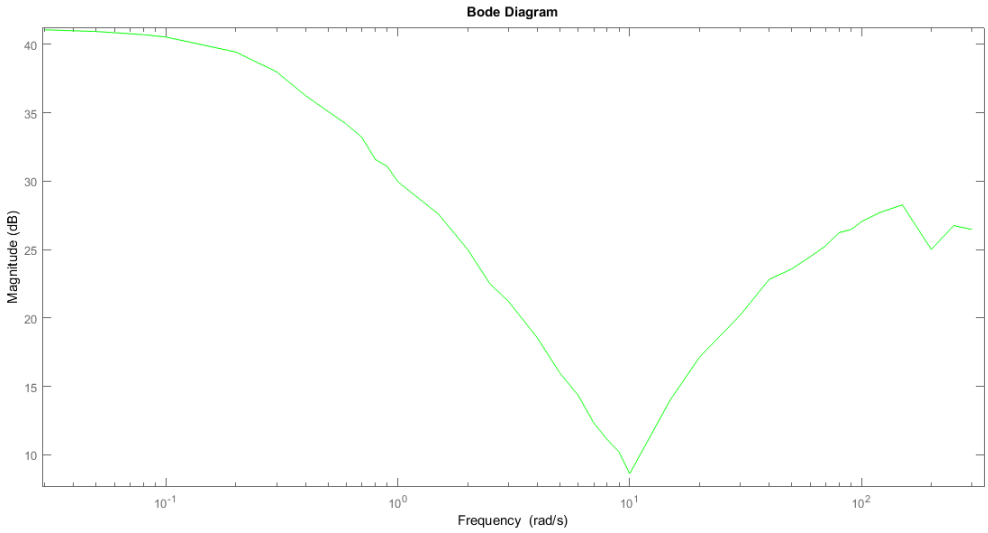

Figure 3.6: Frequency response for extra flexible link model

In this case, both 2 mass and 3 mass spring damper model are used to match the

frequency response of the physical system. The matching results are depicted in figure 3.7

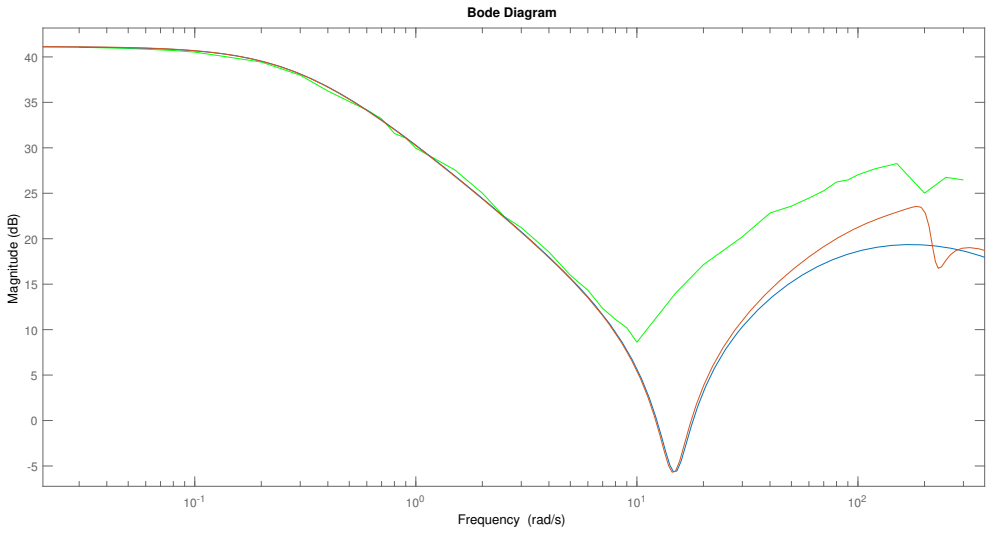

Figure 3.7: Frequency response matching plot using the 2 mass and 3 mass spring damper model. The green line is the extra flexible link physical model bode plot, the blue line is modified matched 2 mass spring damper model, the red line is the modified matched 3 mass spring damper model.

3.4 Feedback PI controller

PID controller is a common control method which is widely used in automation and mechanical process. It is suitable for both linear and nonlinear control systems. The formula for a basic parallel PID controller is[47]:

$$U_c(s) = [k_p + k_i\frac{1}{s} + k_D s]E(s) \tag{3.2}$$

where $U_c(s)$ is the controller output, $E(s)$ is the controller input error, k_p, k_I and k_D are the proportional, integral and derivative individual coefficients. The proportional part can speed up the response and decrease the steady state offset, the integral part can eliminate the steady state offset, the derivative part can be used to tune the damping effect response. Since only the motor velocity is measurable by tachometer and can be feed back to achieve the accurate control of the flexible link, the classical structure based on PI velocity loop controller is applied as the feedback control method[48]:

$$U_c(s) = [k_p + k_i\frac{1}{s}]E(s) \tag{3.3}$$

Figure 3.8 depicts the structure of the PI feedback controller, where in the experiment, the feedback $Y(s)$ is the motor velocity and $U_c(s)$ is the input voltage for Qunaser device.

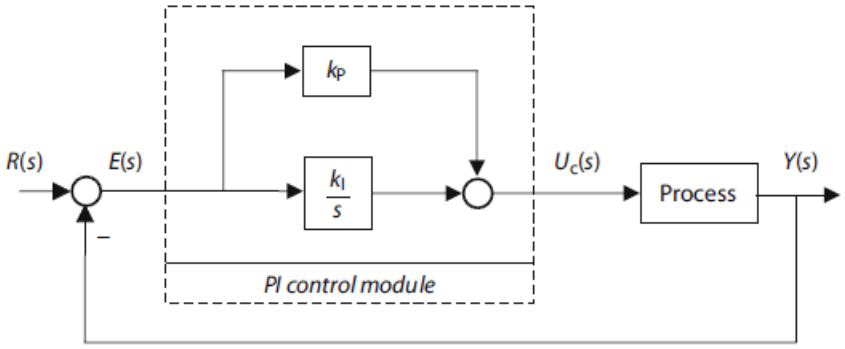

Figure 3.8: A classical structure of the PI feedback controller.[47]

3.5 Filter design and compensation

Filtering is a common tool to process the signal and get the desired data. There are different types of the filter: low pass, high pass, band pass and band stop.[49] Depending on the application one can choose the proper filter.

3.5.1 Low pass filter

The velocity obtained from the tachometer includes also noise which requires to be filtered for more accurate computations. Since the noise is mainly high frequency signal, low pass filter is used to process the signal from the tachometer. A first order low pass filter is a very simple type filter and is easy to design and apply. Through the test, attenuating the signal above $10Hz$ was good enough to remove the noise from the tachometer. Thus a low pass filter with cut-off frequency $10Hz$ can be applied for processing the signal in the experiment. The bode plot of the first order low pass filter is depicted in figure 3.9.

However, the first order low pass filter can cause time delay for the processed signal. Thus the feedback velocity contains a time delay compared with the reference motor velocity. Chapter 4 investigates and discusses the difference between controllers with and without filter compensation.

3.5.2 Notch filter

Band stop filter is a filter that attenuates a special range of frequency without change the other frequencies. A notch filter is a type of band-stop filter with a narrow stop band.[50] Figure 3.10 shows a bode plot of a notch filter with center stop frequency $68rad/s$.

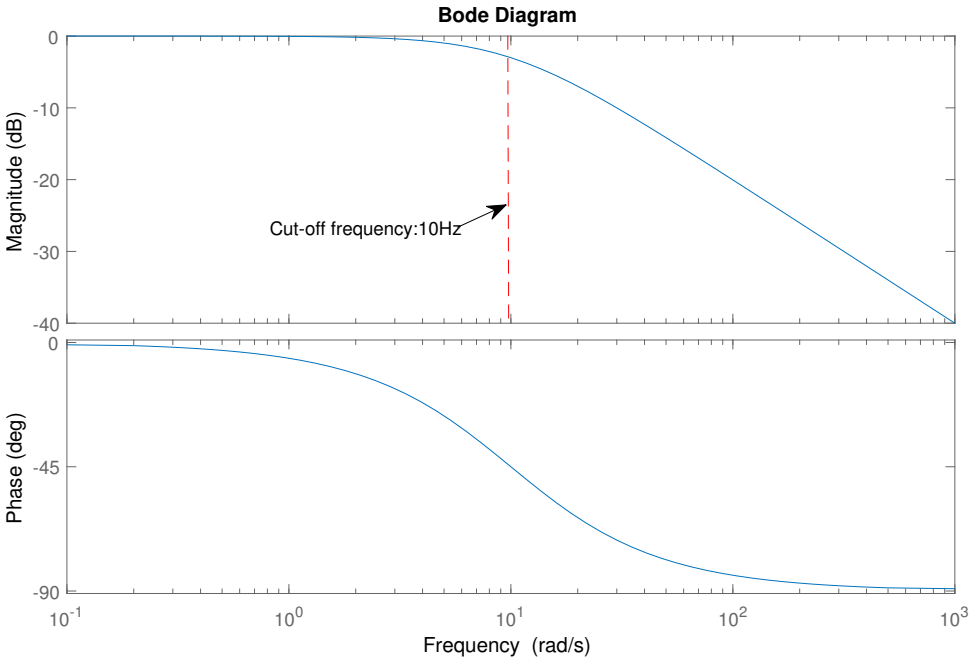

Figure 3.9: Bode plot of the first order low pass filter with cut-off frequency $10Hz$.

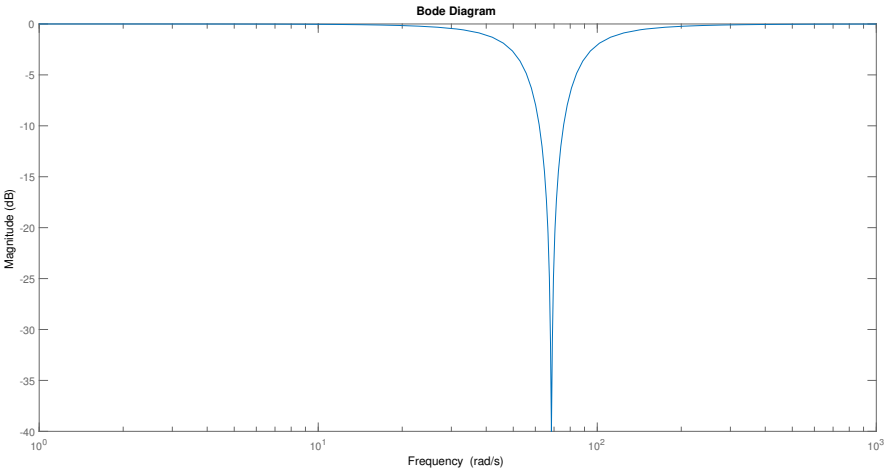

Figure 3.10: Bode plot of the notch filter with center stop frequency $68rad/s$.

4
Results

4.1 Experiment setup

To investigate the performance of the control scheme, two types of the extra link models are mounted on the Quanser SRV02 rotary base unit. One is an extra rigid link with large inertia, another is a flexible link which is fixed by two springs.
In the experiment, the motor velocity measured by the tachometer is used as feedback for the controller. An encoder mounted on the load shaft is used to measure the extra rigid link position. A combination of encoder and potentiometer is used to measure the extra flexible link position and to compare with designed reference trajectory. The PI parameters are tuned by following the rules of thumb. In order to obtain stable and accurate tracking results, the following PI parameters are used to give the proper tracking performance:

$$k_p = 0.5, k_i = 0.5$$

As mentioned in chapter 3.5.1, first order low pass filter is used to process the signal from the tachometer with the cut-off frequency $10Hz$, the formula of the first order low pass filter is:

$$H(s) = \frac{10}{s + 10} \tag{4.1}$$

To process the signal from the encoder and potentiometer, an IIR type filter designed by Quanser is employed.
The proposed control scheme is implemented in MATLAB. There are two devices for voltage control and data Acquisition:

- The Quanser VoltPAQ-X1 which is a single channel, linear voltage-based power amplifier[51].
- The Quanser Q2-USB Data Acquisition Board which provides a cost-efficient, portable data acquisition solution[52].

Together, along with the other two devices, the Quanser SRV02 system is used to carry out the experiment.

4.2 Experiments for different trajectories

In chapter 3.2, it introduces a method for fourth order trajectory planning. Another two reference trajectories are also designed to be implemented during the test. Figure 4.1 and figure 4.2 show that another two trajectories have the same designed position with different running time.

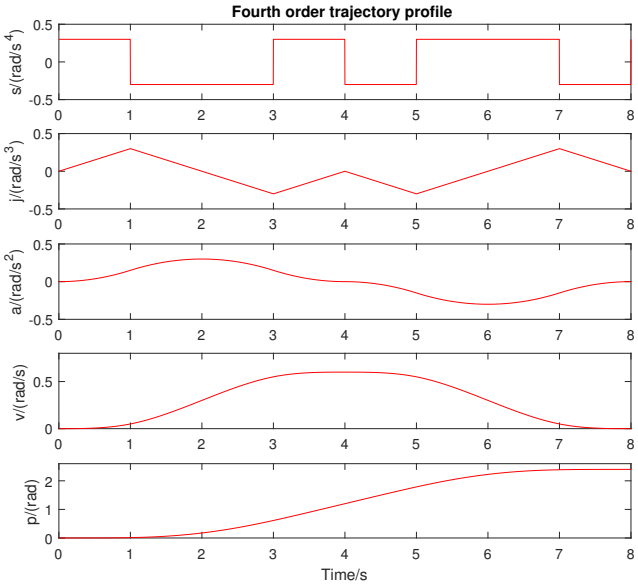

Figure 4.1: Reference trajectory 1.

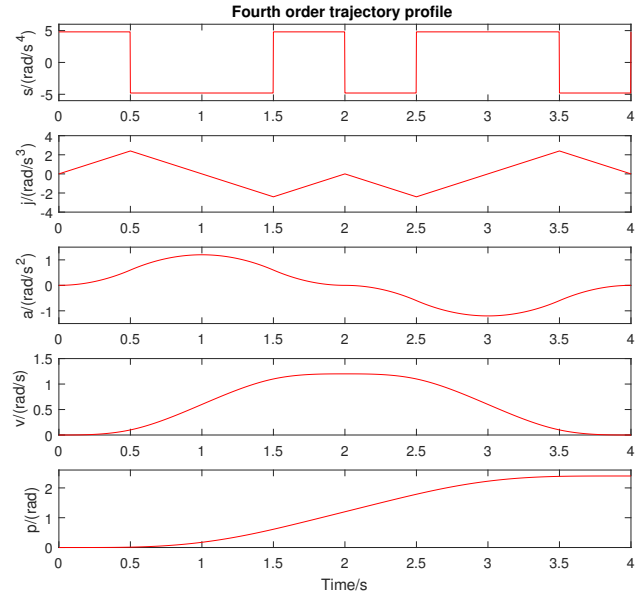

Figure 4.2: Reference trajectory 2.

The test results are depicted in table 4.1. For both rigid link system and flexible link system, feedforward with PI feedback control scheme can achieve better control performance when compared with pure PI feedback controller in all three types of trajectories. It is observed that when the trajectory's frequency increases, both the motor speed error and position error also increases. However, there is no difference using the inverse 3 mass spring damper model for feedforward control comparing to the 2 mass spring damper model. The motor position error is obtained by integrating the motor velocity, thus it seems there is no big difference between only PI feedback control and Feedforward with PI control for the same trajectory.

Table 4.1: The test results for PI feedback control scheme and proposed control scheme(without filter compensation) experiments. The motor speed error and position error are the maximum deviations between the reference motor speed/position and the actual motor speed/position from the experiments.

Physical model	Controller model	Trajectory	Motor speed error (rad/s)	Motor position error (rad)
Rigid link system	Only PI controller	Trajectory 1	2.998	0.2432
		Trajectory 2	7.445	0.3165
		Trajectory 3	23.0545	0.3971
	Feedforward(2 mass) with PI feedback control	Trajectory 1	1.9211	0.1253
		Trajectory 2	3.5810	0.0932
		Trajectory 3	12.1773	0.3464
	Feedforward(3 mass) with PI feedback control	Trajectory 1	1.5863	0.1895
		Trajectory 2	3.9271	0.1141
		Trajectory 3	11.3541	0.2906
Flexible link system	Only PI controller	Trajectory 1	3.4126	0.246
		Trajectory 2	7.455	0.3355
		Trajectory 3	24.8185	0.5459
	Feedforward(2 mass) with PI feedback control	Trajectory 1	2.2705	0.1975
		Trajectory 2	4.3086	0.1322
		Trajectory 3	10.1696	0.3481
	Feedforward(3 mass) with PI feedback control	Trajectory 1	2.4614	0.2390
		Trajectory 2	4.6154	0.2464
		Trajectory 3	15.0353	0.4174

4.3 Experiments with delay compensation

As the results show, it still contains big speed error even applying the feedforward controllers. The main reason is due to the first order low pass filter which causes delay in the feedback. Since the filter model is known, it is easy to compensate for the delay in control scheme. The motor speed error and the link position error are the maximum deviations between the reference value and the measured value. The encoder and potentiometer can measure the link position, thus the link speed is using the derivative of the link position. The experimental results are depicted in table 4.2. The designed reference trajectory for this experiment is only the trajectory 3 of the table 4.1.

Table 4.2: The test results for only PI feedback control scheme and the proposed control scheme(with filter compensation) experiments. The motor and link speed error and link position error are the maximum deviations between the reference speed/position and the actual speed/position from the experiments.

Physical model	Controller model	Motor speed error (rad/s)	Link speed error (rad/s)	link position error
Rigid link system	Only PI controller	4.2304	0.3065	0.2319
	Feedforward(2 mass) with PI feedback control	1.3443	0.2347	0.121
	Feedforward(3 mass) with PI feedback control	1.2189	0.1974	0.1342
Flexible link system	Only PI controller	5.8927	1.0587	0.9435
	Feedforward(2 mass) with PI feedback control	1.5320	0.5842	0.6701
	Feedforward(3 mass) with PI feedback control	1.0039	0.6191	0.6808

As the table 4.2 shows, there is a significant improvement for the motor speed error after the delay compensation. Thus delay compensation is necessary for the experiment. As the table 4.2 shows the feedforward with PI feedback control scheme can attain better control performance than only PI feedback control. Comparing to that of the motor speed error, the link speed error between the flexible link system and rigid link system is larger. Thus the control of the flexible link system is harder than the rigid link system. Figure 4.3 and figure 4.4 display the comparison for the motor speed and the link speed of the rigid link system respectively. Figure 4.5 and figure 4.6 display the comparison for the motor speed and the link speed of the flexible link system respectively. As the figures shown, the mass spring damper model works for flexible link robot arm. However, the link velocity contains an oscillation in figure 4.6. There is not a big difference between 2 mass and 3 mass spring damper model for control results. 3 mass spring damper model need to tune a lot for frequency response matching to obtain stable control parameters. Thus 3 mass spring damper model does not show the merit expected while comparing with 2 mass spring damper model.

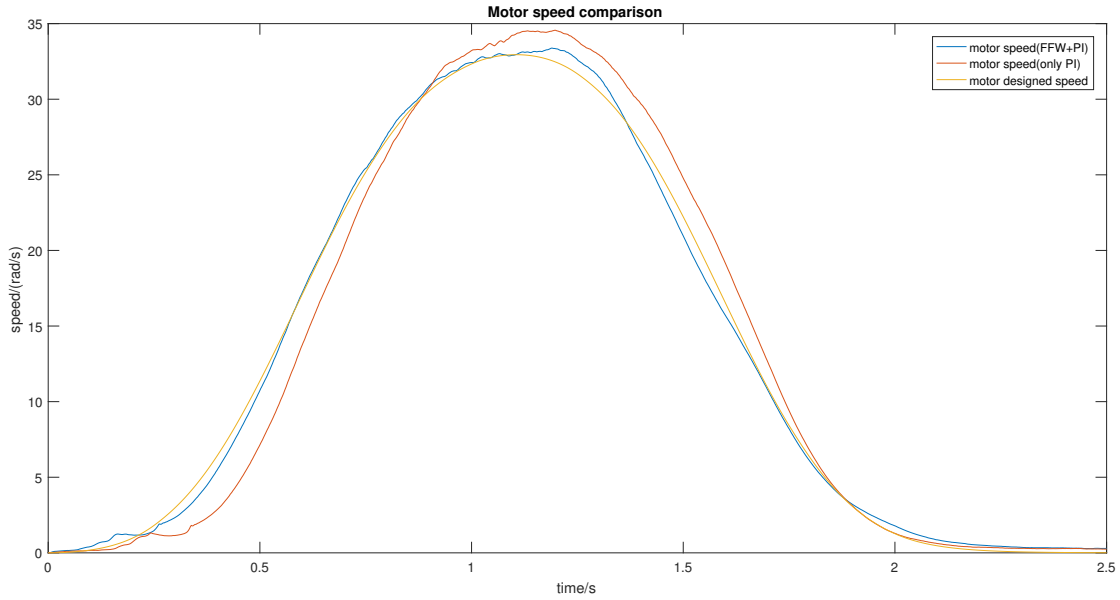

Figure 4.3: Motor speed comparison for the only PI feedback control and feedforward(FFW) with PI feedback control in the rigid link system experiment.

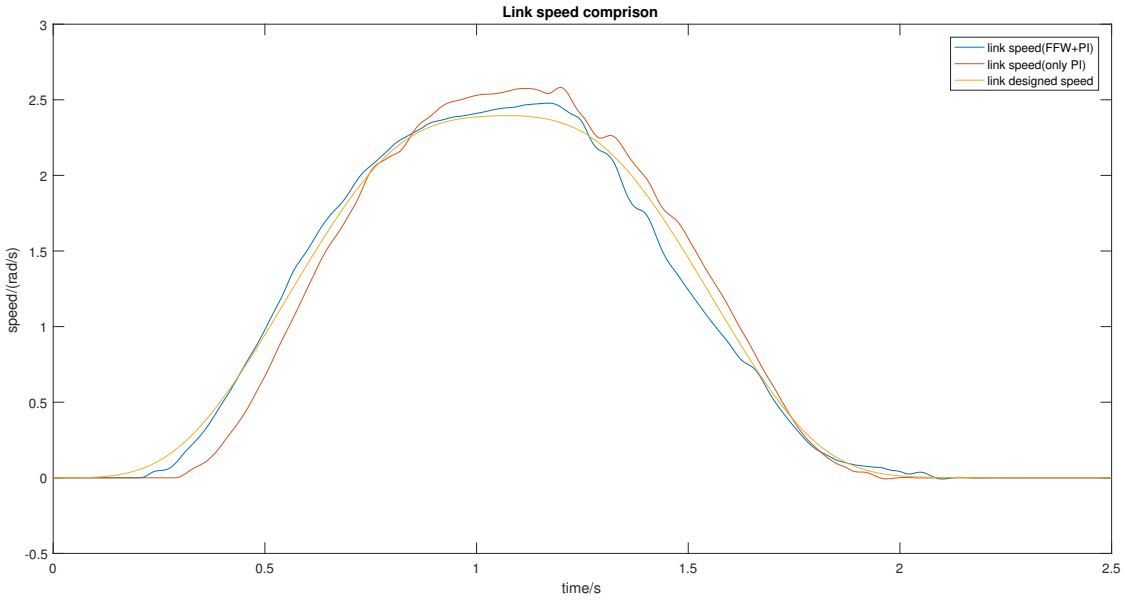

Figure 4.4: Link speed comparison for the only PI feedback control and feedforward(FFW) with PI feedback control in the rigid link system experiment

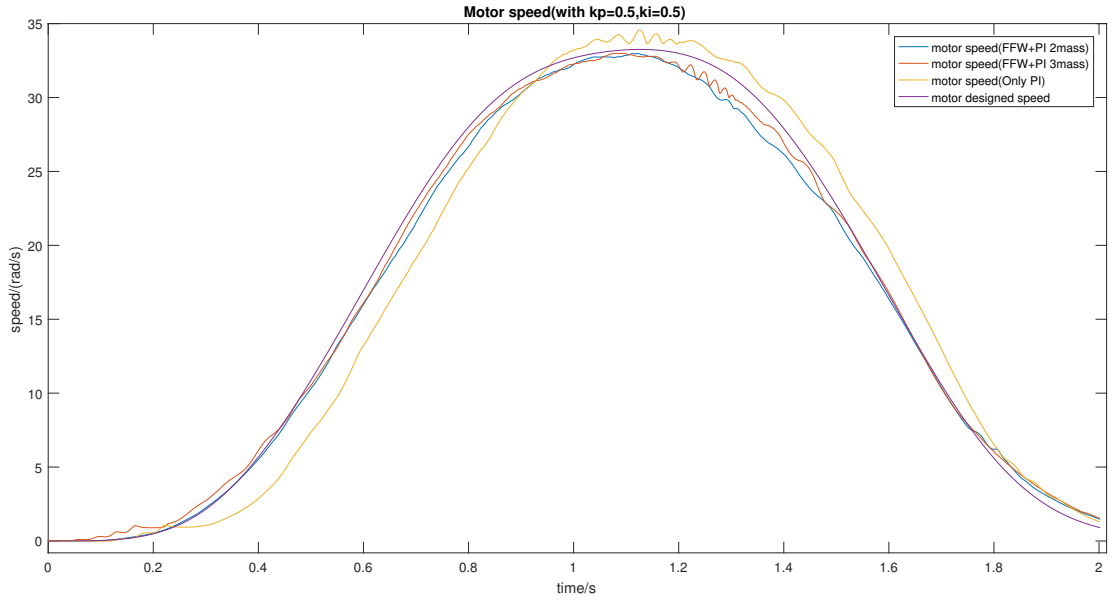

Figure 4.5: Motor speed comparison for the only PI feedback control and feedforward(FFW) with PI feedback control in the flexible link system experiment.Both 2 mass and 3 mass spring damper model results are shown in this graph.

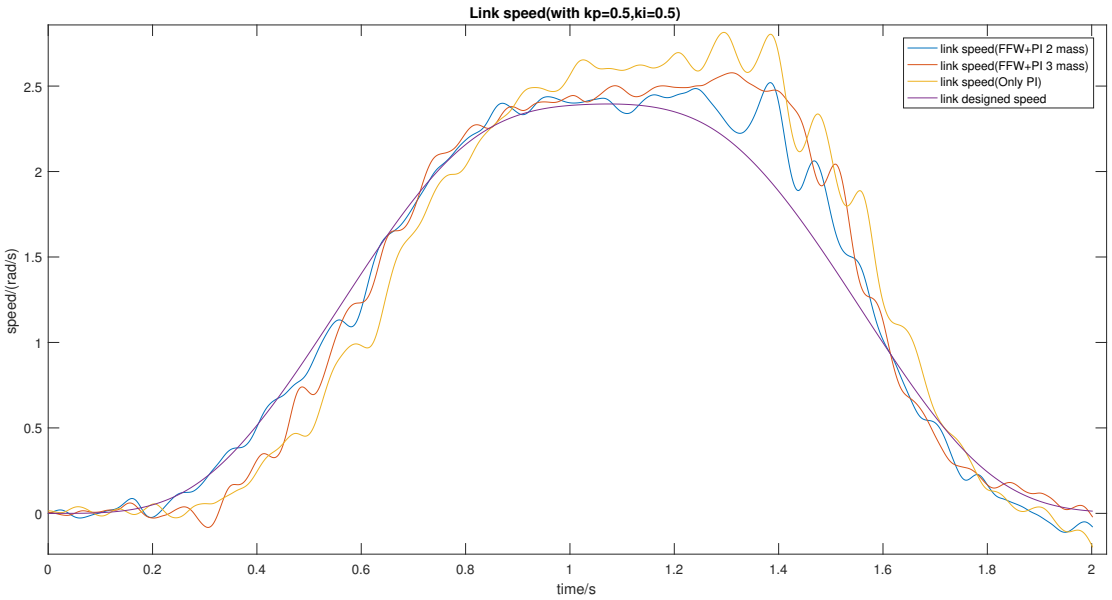

Figure 4.6: Link speed comparison for the only PI feedback control and feedforward(FFW) with PI feedback control in the flexible link system experiment.

4.4 1 mass spring damper model experiment

From the above experiments, there is not a big difference between 2 mass spring damper model and 3 mass spring damper model for the proposed control scheme. To

investigate the spring damper model improves the control performance, an one mass spring damper model is also implemented for the flexible link system experiment. For the 1 mass model, the mathematical model is given in equation (2.10).
Figure 4.7 shows the comparison between the 1 mass model and 2 mass spring damper model for the link velocity in the flexible link system. The feedforward with 2 mass spring damper model can get better results than feedforward with 1 mass model.

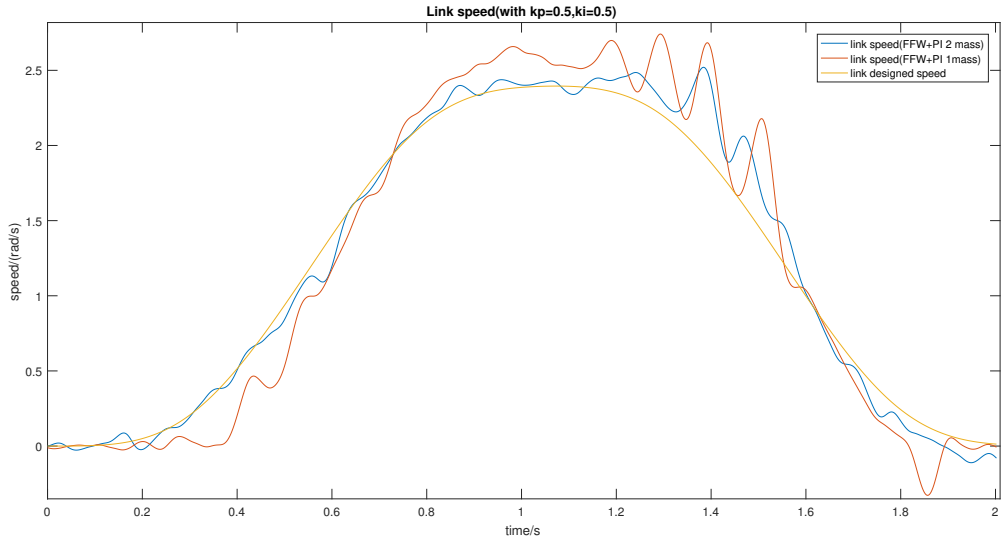

Figure 4.7: Link speed comparison for the 1 mass and 2 mass spring damper model feedforward(FFW) with PI feedback control in the flexible link system experiment.

4.5 Oscillation analysis

The oscillations exist in all flexible link experiments. To investigate the reason of oscillation is due to the control scheme or not, a notch is applied to filtrate the control scheme output voltage. From figure 4.7, the oscillation frequency is found around $68 rad/s$. The notch filter which is described in chapter 3.5.2 is used in the experiment. However, the experiment results still contain the oscillations. The oscillation is not due to the control scheme. That may be caused by the backlash in the motor gearbox.

5

Conclusion and future work

5.1 Conclusion

Flexible link robot arm shows lower energy consumption, safer operation, lower overall mass and in general lower general cost compared with rigid robotic manipulator. One big anomaly of the research on flexible robot is vibration. For most of the real world robotic systems are not verified by the experiment. This thesis implements and evaluates experimentally control schemes as proposed in [6].

The friction has a strong influence on the control scheme. In order to simplify the friction mathematical model, a friction model which combines the Coulomb friction and Viscous friction are used for the system modeling. The spring damper model is introduced to imitate the flexible link and flexible joint. For mass spring damper model, it can simulate resonance and anti-resonance for the flexible link. 2 mass spring damper model and 3 mass spring damper model are presented in this thesis.

Quanser SRV02 is a laboratory platform. It can be used to drive the external link. Two types of external links are mounted in the Quanser SRV02 system: rigid link and flexible link. Then combining with the Quanser SRV02 model, the flexible link robot arm system is obtained.

Giving a sinusoidal input signal and measuring the output signal, the frequency response of the physical system is acquired. The mass spring damper model(2 mass or 3 mass) is used to match the physical system frequency response. However, there exists a backlash inside the motor gearbox and it reduces the resonance and anti-resonance frequency. Thus the effect of the backlash for the physical system should be considered.

After obtaining the matching mass spring damper model, the inverse dynamics of the model can be derived to apply for the feedforward control. Together with a classical structure of PI feedback control, the inverse dynamic computed voltage feedforward control scheme is applied to control the physical system.

For the purpose of implementing feedforward inverse dynamic model work, trajectory planning is essential since the inverse dynamics require that the trajectory's acceleration is continuous derivative. Fourth order trajectory planning with triangular jerk motion profile is used for the design of reference trajectory. Three kinds of trajectories are tested in this experiment. If the trajectory increases frequency which means using the shorter time to get the same position(robot has to move faster), the error for both speed and position would also increase.

In order to remove the noise from the measurement, a first order low pass filter is employed to process the output signal. However, the low pass filter causes a

delay in the feedback. Compensation for the delay is necessary for the accurate control. As the experiment results show, a compensation for the delay in control scheme can improve a lot for the control performance. Comparing to the PI feedback controller, the feedforward with PI feedback control scheme can reduce the error by 30%-40% for both link speed and link position. However, the experiment results do not show that there is merit for using the 3 mass spring damper model as the controller. That may be due to the error in measurements or hardware delay in the experiment, thereby decreasing the prominence of the 3 mass spring damper model controller's merit. Comparing to the 1 mass spring damper model, the 2 mass spring damper model can get better results.

5.2 Future work

To achieve more accurate control of the flexible link robot arm, there are still lots of problems and factors that are needed to be investigated and studied.
In figure 4.6 and figure 4.7, the oscillations exist in the measured flexible link velocities. A notch filter is used to filtrate the control input in this thesis. It has been shown that the oscillation is not due to the control scheme. The backlash or other unidentified reason can cause this oscillation. Thus a further investigation for the oscillation is necessary.
The backlash in the motor gearbox, is an important factors in the physical system and has a strong effect on the flexible link control. There are mainly two ways to reduce the backlash effect: replace the backlash gearbox by anti-backlash gearbox or apply a control method to compensate the backlash. Replacing by a anti-backlash gearbox is an easy way to operate in practice. Sometimes it is difficult to avoid backlash. Thus finding a proper control method for reducing the backlash effect should be investigated.
For the 3 mass spring damper model, the matched parameters need to be tuned to obtain the stable control. Thus analyzing the stability of the control scheme is necessary to achieve stable and safe control.
In order to measure the link position and link velocity values, the flexible link in this thesis experiment is simulated by a link fixed by two springs. This is not exactly a flexible link system. Further research for verifying the control scheme and control performance should use a real flexible link system. Accelerometer or other sensors can be used to measure the link tip position and velocity which can act as a more accurate comparison data.
In this thesis, the control results for proposed control scheme are only compared with a PI feedback controller. However further comparison with other controller is required in order to evaluate the proposed approach with respect to the state of art.

Bibliography

[1] M.O. Tokhi and A.K.M. Azad. *Flexible Robot Manipulators-Modelling, simulation and control*. 2008, The Institution of Engineering and Technology, London, United Kingdom

[2] Jee-Hwan Ryu, Dong-Soo Kwon, B. Hannaford. *Control of a flexible manipulator with noncollocated feedback: time-domain passivity approach*, IEEE Transactions on Robotics, 2004, Volume 20, Issue 4

[3] Yanqing Gao, Fei-Yue Wang, Zhi-Quan Xiao *Flexible Manipulators-Modeling, Analysis, and Optimum Design*, 2013, Elsevier Inc.

[4] Santosha Kumar Dwivedy, Peter Eberhard. *Dynamic analysis of flexible manipulators, a literature review*. Mechanism and Machine Theory 41 (2006) 749–777

[5] R.J. Theodore, A. Ghosal, *Comparison of the assumed modes and finite element models for flexible multi-link manipulators*. The International Journal of Robotics Research 14 (2) (1995) 91–111.

[6] Mazin Hamad, *Modelling and Feed-Forward Control of Robot Arms with Flexible Joints and Flexible Links*. Chalmers University of Technology, 2016.

[7] M. Benosman and G. Le Vey, *Control of flexible manipulators: A survey*. Robotica, 10/2004, Volume 22, Issue 5

[8] Gerasimos G.Rigatos, *Model-based and model-free control of flexible-link robots: A comparison between representative methods*. Applied Mathematical Modelling, 2009, Volume 33, Issue 10

[9] R.H. Cannon, E. Schmitz *Initial experiments on end-point control of a flexible one-link robot*, The International Journal of Robotics Research 3 (3) (1984) 62–75

[10] F. Rakhsha, A.A. Goldenberg, *Dynamic modeling of a single link flexible robot*, Proceedings of the IEEE International Conference on Robotics and Automation (1985) 984–989

[11] E. Barbieri, U. Ozguner, *Unconstrained and Constrained Mode Expansions for a Flexible Slewing Link*, American Control Conference, 1988

[12] J.N Bricout, J.C Debus, P Micheau, *A finite element model for the dynamics of flexible manipulators*, Mechanism and Machine Theory, Vol. 25, No. I, pp. 119-128, 1990

[13] H. C. Moulin, E. Bayo, *Accuracy of discrete models for the solution of the inverse dynamics problem for flexible arms, feasible trajectories*, Journal of Dynamic Systems, Measurement and Control, Transactions of the ASME, 09/1997

[14] Z. Mohamed, M.O. Tokhi, *Command shaping techniques for vibration control of a flexible robot manipulator*, Mechatronics 14 (2004) 69–90

[15] G. Zhu,S.S Ge,T.H Lee, *Simulation studies of tip tracking control of a single-link flexible robot based on a lumped model*, Robotica(1999), Volume 17, 71–78.

[16] S. M. Megahed, K. T. Hamza, *Modeling and simulation of planar flexible link manipulators with rigid tip connections to revolute joints*, Robotica(2004), Volume 22, 285-300.

[17] W. Khalil, M. Gautier, *Modeling of mechanical systems with lumped elasticity*, Proceedings 2000 ICRA. Millennium Conference. IEEE International Conference on Robotics and Automation, 2000

[18] Dirk Nissing, *A vibration damped flexible robot: identification and parameter optimization*, Proceedings of the 2000 American Control Conference, 2000

[19] H. Asada, J.H. Park, S. Rai, *A control-configured flexible arm: integrated structure control design*, Robotics and Automation, 1991. Proceedings. 1991 IEEE International Conference.

[20] C.H. Menq, J.S. Chen, *Dynamic modeling and payload-adaptive control of a flexible manipulator*, Robotics and Automation, 1988. Proceedings. IEEE International Conference

[21] G. Feng, M. Palaniswami, *Adaptive control of partially known single-link flexible manipulators*, Fifth International Conference on Advanced Robotics 'Robots in Unstructured Environments, 1991, 1784 - 1787 vol.2

[22] Tzung-Cheng Yang, J.C.S. Yang, P. Kudva, *Adaptive control of a single-link flexible manipulator with unknown load*, IEEE Proceedings D: Control Theory and Applications, 03/1991, Volume 138, Issue 2

[23] V.V. Korolov, Y.H. Chen, *Robust control of a flexible manipulator arm*, Proceedings. 1988 IEEE International Conference on Robotics and Automation

[24] P. Misra, *Robust control of flexible manipulators*, IEEE 1989 International Conference on Systems Engineering

[25] K.S. Rattan ; V. Feliu, *A robust control scheme for flexible manipulators*, Proceedings of the IEEE 1991 National Aerospace and Electronics Conference

[26] S. Pal, H.E. Stephanou, G. Cook, *Optimal control of a single link flexible manipulator*, Proceedings. 1988 IEEE International Conference on Robotics and Automation

[27] X.D. Ji, B.O. Familoni, *Implementation of self-tuning control of a flexible manipulator system*, Proceedings of 1994 American Control Conference

[28] O. Morgul, *On the boundary control of a flexible robot arm*, Proceedings of the 40th IEEE Conference on Decision and Control

[29] P.T. Kotnik, S. Yurkovich, U. Ozguner, *Acceleration feedback control for a flexible manipulator arm*, Journal of Robotic Systems, 1988, Volume 5, Issue 3

[30] Jalili, Nader, *An infinite dimensional distributed base controller for regulation of flexible robot arms*, Journal of Dynamic Systems, Measurement and Control, Transactions of the ASME, 12/2001, Volume 123, Issue 4

[31] L.B. Gutierrez, F.L. Lewis, J.A. Lowe, *Implementation of a neural network tracking controller for a single flexible link: comparison with PD and PID controllers*, IEEE Transactions on Industrial Electronics, 1998, Volume 45, Issue 2

[32] K.S. Rattan, V. Feliu, *Feedforward control of flexible manipulators*, Proceedings 1992 IEEE International Conference on Robotics and Automation

[33] D. Isobe, A. Kato, *FEEDFORWARD CONTROL OF FLEXIBLE LINK SYSTEMS USING PARALLEL SOLUTION SCHEME*, International Journal of Robotics and Automation, 2008, Volume 23, Issue 1

[34] A. Abe, K. Hashimoto, *A novel feedforward control technique for a flexible dual manipulator*, ROBOTICS AND COMPUTER-INTEGRATED MANUFACTURING, 10/2015, Volume 35

[35] Carlos E. Padilla, *Performance Limits and Robustness Issues in the Control of Flexible Link Manipulators*, PhD thesis, Department of Aeronautics and Astronautics, M.I.T., 1992.

[36] Quanser. *USER MANUAL-SRV02 Rotary Servo Base Unit*, 2015 .

[37] J. Apkarian, M. Lévis, H. Gurocak, *Instructor Workbook-SRVV02 base unit Experiment For Matlab/simulink users*, 2011 Quanser Inc.

[38] Ivan Virgala, Peter Frankovský, and Mária Kenderová. *Friction Effect Analysis of a DC Motor*. American Journal of Mechanical Engineering, 2013, Vol. 1, No. 1, 1-5

[39] Module 7.1: Frequency Response
`http://homepages.ed.ac.uk/jwp/control06/controlcourse/restricted/course/advanced/module7-1.html`

[40] Keesman K.J. (2011) *System Response Methods*. In: System Identification. Advanced Textbooks in Control and Signal Processing. Springer, London

[41] J.H.Baek, Y.K.Kwak, S.H.Kim. *On the frequency bandwidth change of a servo system with a gear reducer due to backlash and motor input voltage*. Archive of Applied Mechanics, 73 (2003), 367–376

[42] J.H.Baek, Y.K.Kwak, S.H.Kim (2003). *Analysis on the Influence of Backlash and Motor Input Voltage in Geared Servo System*

[43] Boerlage, M; Steinbuch, M; Lambrechts, Pvan de Wal, M. *Model-based feedforward for motion systems*. Proceedings of 2003 IEEE Conference on Control Applications, 2003.

[44] Paul Lambrechts, Matthijs Boerlage, Maarten Steinbuch. *Trajectory planning and feedforward design for electromechanical motion systems*. Control Engineering Practice 13 (2005) 145–157

[45] Paul Lambrechts, Matthijs Boerlage, Maarten Steinbuch. *Trajectory Planning and Feedforward Design for High Performance Motion Systems*. Proceeding of the 2004 American Control Conference, Boston, Marrachusens June 30 -July 2,2004

[46] L. Biagiotti and C. Melchiorri. *Trajectory Planning for Automatic Machines and Robots* Springer Berlin Heidelberg 2008, Germany

[47] Michael A. Johnson and Mohammad H.Moradi(Editors). *PID Control-New Identification and Design Methods*. Springer, 2005

[48] Rafael Kelly,Javier Moreno *Learning PID Structures in an Introductory Course of Automatic Control*. IEEE TRANSACTIONS ON EDUCATION, VOL. 44, NO. 4, NOVEMBER 2001

[49] Stefan Niewiadomski. *Filter Handbook-A Practical Design Guide*. 1989 Elsevier Ltd.

[50] ChunMei WANG, WeiCai XIAO. *Second-order IIR Notch Filter Design and implementation of digital signal processing system.* Applied Mechanics and Materials Vols. 347-350 (2013) pp 729-732
[51] Quanser. *VoltPAQ-X1 Amplifier-User manual*,2012.
[52] Quanser. *Q2-USB Dta Acquisition Board-User manual*,2012.

A

Frequency response identification data

Here are two tables to show the collected data for the physical system frequency response. Table A.1 displays the collected data for the rigid link robot system and table A.2 displays the collected data for flexible link robot system. For the rigid link robot system, the input frequency used the unit Hz. While for the flexible link robot system, the input frequency used the unit rad/s. The relation between them is: $\omega = 2\pi f$, where ω with unit rad/s and f with unit Hz. The bode plots for both rigid link and flexible link robot system are shown in figure 2.8 and figure 3.6.

Table A.1: Collected frequency response data for rigid link robot system.

Frequency(Hz)	Amplitude(v)	Maximum motor speed(rad/s)	Gain (db)
0.02	2	230.8032	41.7122
0.03	2	230.1042	41.6858
0.04	2	228.0796	41.6091
0.05	2	223.6116	41.4372
0.06	2	219.9115	41.2923
0.07	2	213.4189	41.0320
0.08	2	207.9734	40.8075
0.09	2	201.4808	40.5320
0.1	2	195.3372	40.2631
0.2	2	141.7905	37.4803
0.3	2	105.3481	34.8999
0.4	2	82.5192	32.7785
0.5	2	67.4954	31.0328
0.6	2	55.5643	29.3433
0.7	2	48.0664	28.0842
0.8	2	40.9105	26.6841
0.9	2	34.7739	25.2724
1.0	2	30.3338	24.0859
1.5	2	16.3712	18.7290
2.0	2	20.1132	20.5170
3.0	2	32.3793	24.6527
4.0	2	39.5422	26.3886
5.0	2	41.9298	26.8978
6.0	2	45.0016	27.5119
7.0	2	47.3822	27.9597
8.0	2	48.7436	28.2057
9.0	2	51.8223	28.7377
10.0	2	51.8153	28.7365
15.0	2	54.4613	29.1691
20.0	2	52.1574	28.7937
30.0	2	61.7218	30.2561
40.0	2	48.7505	28.2069
50.0	2	41.5877	26.8267

Table A.2: Collected frequency response data for flexible link robot system.

Frequency(rad/s)	Amplitude(v)	Maximum motor speed(rad/s)	Gain (db)
0.03	2	214.1170	41.0604
0.05	2	211.0452	40.9349
0.08	2	205.5300	40.7049
0.1	2	201.4808	40.5320
0.2	2	177.6047	39.4364
0.3	2	150.3078	37.9870
0.4	2	123.0806	36.2512
0.5	2	107.7217	35.0934
0.6	2	96.8309	34.1676
0.7	2	86.5683	33.1945
0.8	2	71.9076	31.5828
0.9	2	67.8375	31.0767
1.0	2	59.6554	29.9603
1.5	2	45.3367	27.5764
2.0	2	33.7477	25.0122
2.5	2	25.2235	22.4835
3.0	2	21.8166	21.2231
4.0	2	16.0221	18.5418
5.0	2	11.9311	15.9809
6.0	2	9.8855	14.3474
7.0	2	7.8400	12.3337
8.0	2	6.8180	11.1204
9.0	2	6.1359	10.2049
10.0	2	5.1131	8.6211
15.0	2	9.5435	14.0415
20.0	2	13.6345	17.1401
30.0	2	19.4290	20.2164
40.0	2	26.2498	22.8299
50.0	2	28.6374	23.5860
60.0	2	31.7022	24.4691
70.0	2	34.7739	25.2724
80.0	2	38.8650	26.2385
90.0	2	39.8843	26.4634
100.0	2	42.6140	27.0384
120.0	2	46.0208	27.7064
150.0	2	49.0856	28.2664
200.0	2	33.7477	25.0122
250.0	2	41.2456	26.7549
300.0	2	39.8843	26.4634

B

Frequency response matched results of the mass spring damper model

B.1 Matched results for rigid link robot system

Table B.1 and table B.2 show the frequency response matched results for rigid link robot arm by applying 2 mass and 3 mass spring damper model.

Table B.1: Matched 2 mass spring damper model parameters' results for rigid link robot system.

Symbol	Definition	Value
J_a	Gearbox(or flexible link) inertia	4.81×10^{-5}
d_a	Gearbox(or flexible link) damping	3×10^{-5}
k_a	Gearbox(or flexible link) stiffness	1.2×10^{-2}
B_a	Gearbox viscous friction	1.68×10^{-6}

Table B.2: Matched 3 mass spring damper model parameters' results for rigid link robot system.

Symbol	Definition	Value
J_a	Gearbox(or flexible link) inertia	0.8099×10^{-5}
d_a	Gearbox(or flexible link) damping	5×10^{-5}
k_a	Gearbox(or flexible link) stiffness	0.01
J_l	The extra link inertia	4.5099×10^{-5}
d_l	The extra link damping	5.4×10^{-4}
k_l	The extra link stiffness	0.5
B_l	The extra link viscous friction	1.95×10^{-6}

B.2 Matched results for flexible link robot system

Table B.3 and table B.4 show the frequency response matched results for flexible link robot arm by applying 2 mass and 3 mass spring damper model.

Table B.3: Matched 2 mass spring damper model parameters' results for flexible link robot system.

Symbol	Definition	Value
J_a	Gearbox(or flexible link) inertia	4.91×10^{-5}
d_a	Gearbox(or flexible link) damping	2×10^{-4}
k_a	Gearbox(or flexible link) stiffness	1.3×10^{-2}
B_a	Gearbox viscous friction	1.98×10^{-6}

Table B.4: Matched 3 mass spring damper model parameters' results for flexible link robot system.

Symbol	Definition	Value
J_a	Gearbox(or flexible link) inertia	2.96×10^{-6}
d_a	Gearbox(or flexible link) damping	1.2×10^{-4}
k_a	Gearbox(or flexible link) stiffness	0.013
J_l	The extra link inertia	2.995×10^{-5}
d_l	The extra link damping	2×10^{-4}
k_l	The extra link stiffness	1.02
B_l	The extra link viscous friction	9.05×10^{-7}

C

1 mass spring damper model frequency response matching

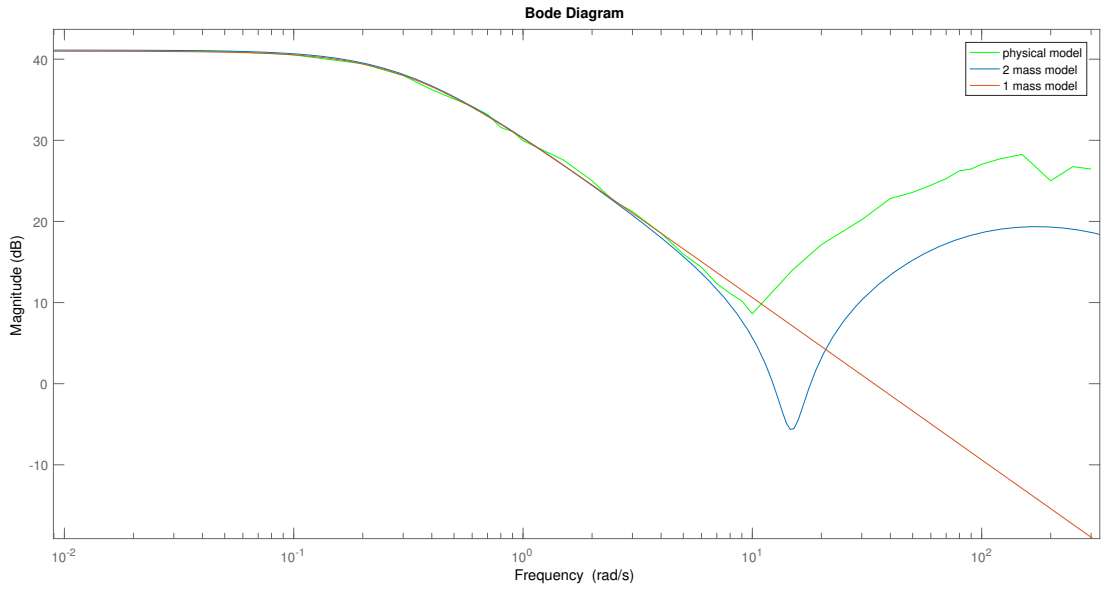

Figure C.1: The frequency response matching using the 1 mass spring damper model. The green line is the physical model frequency response, the blue line is the 2 mass model frequency response and the red line is the 1 mass model frequency response.

D

Detailed control scheme

Figure D.1 describes a detailed control scheme based on mass spring damper model.

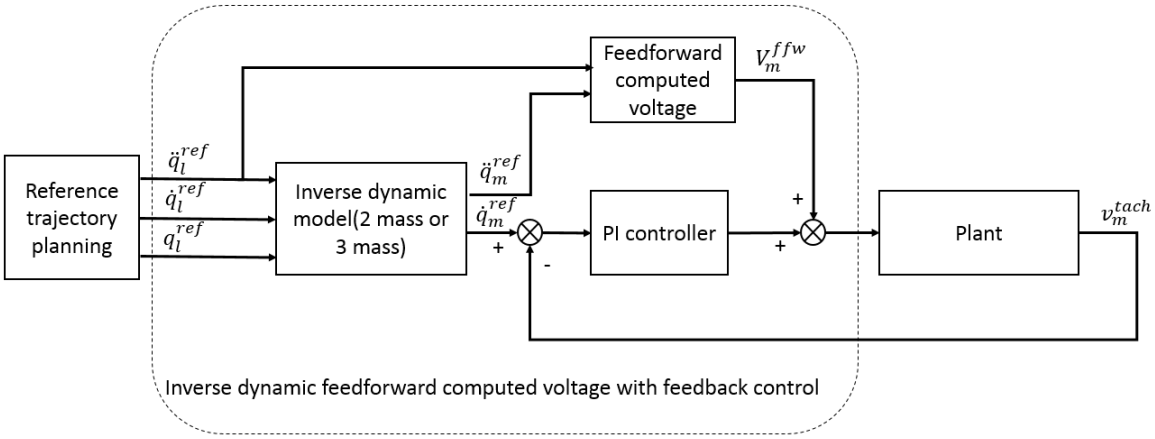

Figure D.1: Inverse dynamic feedforward computed voltage control with PI feedback control scheme.